DISSERTATIONES
CHIMICAE
UNIVERSITATIS
TARTUENSIS
165

SIIM KUKK

Kinetic aspects of interaction between dopamine transporter and *N*-substituted nortropane derivatives

DISSERTATIONES CHIMICAE UNIVERSITATIS TARTUENSIS
165

DISSERTATIONES CHIMICAE UNIVERSITATIS TARTUENSIS
165

SIIM KUKK

Kinetic aspects of interaction between dopamine transporter and *N*-substituted nortropane derivatives

UNIVERSITY OF TARTU
Press

Institute of Chemistry, Faculty of Science and Technology, University of Tartu, Estonia

Dissertation was accepted for the commencement of the degree of *Doctor philosophiae* in Chemistry at the University of Tartu on June 14th, 2017 by the Council of Institute of Chemistry, Faculty of Science and Technology, University of Tartu.

Supervisor:	Professor Jaak Järv Institute of Chemistry, University of Tartu, Estonia
Opponent:	Magnus Schou, Ph.D, Associate Principal Scientist Department of Clinical Neuroscience, Karolinska Institutet, Sweden
Commencement:	August 29, 2017 at 10:00 Ravila 14A-1021, Tartu

This work was funded by the Estonian Ministry of Education and Science (IUT 20–15).
This work was supported by Graduate School of Functional materials and technologies receiving funding from the European Regional Development Fund in University of Tartu, Estonia.

ISSN 1406-0299
ISBN 978-9949-77-513-2 (print)
ISBN 978-9949-77-514-9 (pdf)

University of Tartu Press
www.tyk.ee

CONTENTS

LIST OF ORIGINAL PUBLICATIONS

I Kukk, S.; Stepanov, V.; Järv, J. Thermal Stability of Dopamine Transporters. *J. Membr. Biol.* **2015,** 248, 775–781. https://doi.org/10.1007/s00232-015-9794-9

II Kukk, S.; Järv, J. Differentiating between drugs with short and long residence times. *MedChemComm*. **2016**, 7, 1654–1656. https://doi.org/10.1039/C6MD00269B

III Kukk, S.; Miidla, P.; Järv, J. Kinetic tools for the identification of ligand-receptor interaction mechanisms. *Proc. Est. Acad. Sci.* **2017**, 66, 202–213. https://doi.org/10.3176/proc.2017.2.08

IV Kukk, S; Järv, J. Synthesis and dopamine transporter binding kinetics of a series of *N*-substituted nortropane derivatives. *Bioorg. Med. Chem. Lett. Submitted*.

Author's contribution:

I The author performed most of the experiments, was responsible for writing and submitting the manuscript.

II The author performed all the experiments, was responsible for writing and submitting the manuscript.

III The author derived the model, wrote the code and performed the simulations, and was responsible for writing and submitting the manuscript.

IV The author prepared all compounds, performed all experiments and was responsible for writing and submitting the manuscript.

ABBREVIATIONS

Ala	Alanine
Asp	Aspartic acid
BTCP	1-[1-(2-Benzo[*b*]thienyl)cyclohexylpiperidine
CFT	2β-Carbomethoxy-3β-(4'-fluorophenyl)tropane
CPM	Counts per minute
dDAT	Drosophila melanogaster dopamine transporter
DAT	Dopamine transporter
DiPEA	*N*,*N*-Diisopropylethylamine
E_a	Activation energy
FP	Fluoropropyl
GBR12909	1-(2-[Bis(4-Fluorophenyl)methoxy]ethyl)-4-(3-phenylpropyl)piperazine
HEPES	4-(2-Hydroxyethyl)piperazine-1-ethanesulfonic acid
HPLC	High-performance liquid chromatography
IC_{50}	The median concentration of an inhibitor that causes 50% inhibition of a given system
k_i	Isomerization on-rate constant
k_{-i}	Isomerization off-rate constant
k_{inact}	Inactivation rate constant
K_i	Inhibition constant
K_{isom}	Isomerization constant
K_L	Dissociation constant of the initial binding
LeuT	Leucine transporter
NBS	*N*-Bromosuccinimide
NET	Norepinephrine transporter
PE2I	*N*-(3-Iodoprop-(2*E*)-enyl)-2β-carbomethoxy-3β-(4'-methylphenyl)nortropane
PET	Positron emission tomography
Phe	Phenylalanine
POPC	1-Palmitoyl-2-oleoyl-*sn*-glycero-3-phosphocholine
RTI	Research Triangle Institute
SEM	Standard error of the mean
SERT	Serotonin transporter
SPECT	Single photon emission computed tomography
SPR	Surface plasmon resonance

Ser	Serine
SLC6	Solute carrier 6 gene family
TEA	Triethylamine
TFA	Trifluoroacetic acid
THF	Tetrahydrofuran
Tyr	Tyrosine
Val	Valine
WIN35,428	2β-Carbomethoxy-3β-(4'-fluorophenyl)tropane
WIN	Winthrop

INTRODUCTION

Dopamine transporter (DAT) is a 12-transmembrane protein, belonging to a neurotransmitter-sodium symporter family, responsible for the uptake of dopamine from postsynaptic cleft and is widely expressed in mammalian brain. DAT is target for various therapeutic drugs used for treatment of psychiatric diseases and disorders, e.g. depression, anxiety, attention deficit hyperactivity and epilepsy. Several psychostimulants, like cocaine or amphetamine, also target monoamine transporters, including DAT.[1] One of the driving forces for DAT study is the search for specific ligands which inhibit the binding of cocaine, or its analogues, while maintaining the transport of substrate.

Langley reported in 1905 that nicotine and curare caused tonic contraction in the muscles of frog legs long after nerve section.[2,3] The phenomenon was further mathematically described by Archibald Hill in 1909, who reported that the time-curves of muscle twitching, when muscles were submerged in the solution of nicotine, followed an exponential function.[4] This was one of the first studies of drug action kinetics, although the target protein was not identified. Nowadays it is known that the effect was caused by the binding of nicotine to nicotinic acetylcholine receptor.[5,6] Publication of reports on protein-ligand interaction kinetics accelerated in the 1970s with thorough investigation of nicotinic acetylcholine receptor agonists and antagonists.[7,8]

Strickland, Palmer and Massey proposed a two-step protein-ligand interaction model, where the overall dissociation constant is determined by two subsequent equilibria.[9] Modulation of these equilibria allows enhancement of the apparent drug affinity. However, this option has not been discussed and considered widely. One of the possible reasons is that the presence of the second step in binding process can be identified only by kinetic experiments, and the one- and two-step interaction mechanisms cannot be differentiated by standard displacement studies. Since that time kinetic approach has been used to characterize the binding mechanism and rate constants of the slow step of numerous ligand-protein systems, including muscarinic acetylcholine receptor,[10,11] dopamine receptor[12] and dopamine transporter[13,14].

In 2006 Copeland and others introduced a simplified metric, drug residence time, to characterize the slow drug-target off-rate.[15] Although drug residence time, defined as the reciprocal of the off-rate kinetic constant, lacks a clear physical meaning, it could be easily determined by *in vitro* assay methods and used in drug development.[16] Also, it has highlighted the importance of slow ligand off-rate, and therefore, ligand-protein interaction kinetics should be recognized as a crucial part of a lead compound optimization process in drug discovery.[17]

Ideally, the kinetic parameters of a ligand-protein interaction should be determined experimentally for each compound under investigation. Since labeling of every compound of interest is not feasible, an indirect method is used, where the influence of an unlabeled ligand on the binding kinetics of a

single labeled ligand is studied. Therefore, the same reporter ligand can be used for kinetic studies of a series of unlabeled ligands and this has made the kinetic approach effective and comparable with the well-known ligand displacement method.

In this study, the kinetic analysis of DAT interaction with ligands was implemented to study the interaction of a series of *N*-substituted 2β-carbomethoxy-3β-(4'-methylphenyl)-nortropanes with this protein by using a selective DAT ligand [^{3}H]PE2I as the reporter ligand.

In parallel with kinetic study of ligand-DAT interaction mechanism, stability of the membrane-integrated protein and its thermal inactivation kinetics were investigated to consider these results in the planning of kinetic experiments. This study clearly pointed out that the role of membrane environment of the protein cannot be overestimated in explanation of its properties.

LITERATURE OVERVIEW

Dopamine transporter

Dopamine transporter (DAT) belongs to a family of sodium-neurotransmitter symporters, i.e. Na^+ is transported in the same direction as substrates, with other neurotransmitter and amino acid transporters.[18] The solute carrier 6 (SLC6) transporter family has been divided into the following subfamilies on the basis of similarity: monoamine, amino acid, γ-aminobutyric acid and amino acid/ orphan. SLC6 family itself belongs to a solute carrier superfamily consisting of approximately 350 transporters. In addition to being targets of numerous medications, the monoamine transporters of dopamine, norepinephrine (NET) and serotonin (SERT) are targets for some of the most widely used drugs of abuse, e.g. cocaine, amphetamine/methamphetamine and methylenedioxymethamphetamine.[1] Transgenic models give a simplified overview of the role of dopamine transporter. DAT-knockout mouse models have shown a fourfold increase in extracellular dopamine concentrations leading to dopamine dysregulation, which in turn causes hyperlocomotion, impaired cognition and other behavioral impairment.[19] On the contrary, DAT overexpression increases dopamine uptake by half, decreases the extracellular dopamine concentrations and dopamine release by half giving rise to loss of dopamine neurons causing fine motor deficits in mice.[19] DAT function is associated with several proteins, including phosphatases, G protein-coupled receptors, receptor tyrosine kinases, cytosolic kinases, membrane trafficking and scaffolding proteins.[20,21] Interactions between these proteins and DAT are thought to alter surface expression of DAT and regulate DAT functions, e.g. reverse transport.[20]

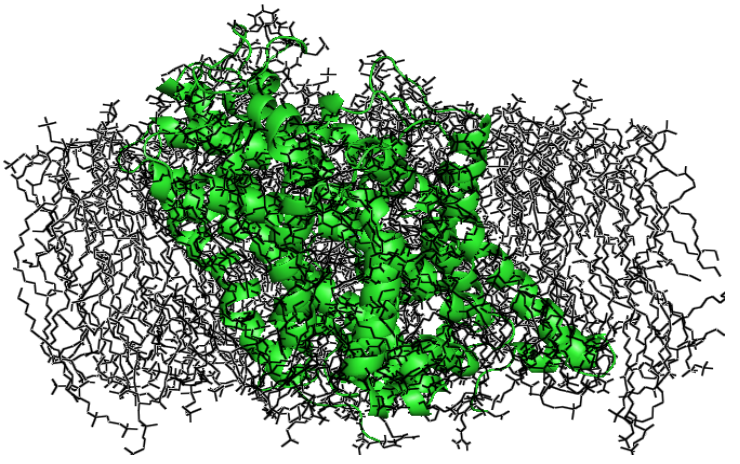

Figure 1. Dopamine transporter (green ribbon) obtained from protein database (4M48).[26] All stabilizing compounds are removed from this structure and phospholipid (POPC) shell is introduced.

In order to understand the molecular mechanisms of transporter action, its detailed structure would be a necessity. The determination of transmembrane leucine transporter (LeuT) structure gave information about the possible structure of DAT,[22] and on the basis of LeuT structure, several DAT-ligand docking simulations have been reported.[23–25] These studies revealed potential substrate and inhibitor binding sites. After publishing *Drosophila melanogaster* DAT crystal structure[26] (Figure 1), a more detailed binding modelling of the protein, as well as binding sites of known inhibitors and substrates which are important for screening of new drug candidates, has been published.[27] Recent findings verify previous results, obtained from LeuT structure.[23,28] These results indicated that the dopamine binding site overlaps with the binding sites of cocaine and its analogues. This postulate contradicts a LeuT structure based DAT simulation study,[25] reporting that the dopamine and cocaine binding sites do not overlap, but are in close proximity. In addition, cocaine can always bind to DAT, whether dopamine has already been bound or not, although DAT affinity for it decreases.[25] The binding of non-catecholic DAT substrate-like inhibitors, amphetamines, is also explained by their interaction at the central dopamine binding site, despite the fact that these ligands omit hydroxyl groups, which are important structure fragments of dopamine (Scheme 1).[23]

Crystallization studies of ligand-DAT complexes also reveal information about the amino acids making up the binding pocket. The amine group of tropane derivatives (Scheme 2) forms a salt bridge with Asp46 and the phenyl group is attracted by the aromatic interaction with Phe325 in dDAT.[28] This indicates the necessity of nitrogen, or any other hydrogen bond acceptor, and phenyl group in DAT ligands. Superposition of β-CFT-dDAT, β-CIT-dDAT and cocaine-dDAT reveals that these ligands (Scheme 2) overlap almost entirely. The benzoate group of cocaine and the halide-substituted phenyl groups of β-CIT and β-CFT form van der Waals interactions with Ser422, Phe325, Tyr124, Val120 and Ala117 in the binding site.[23,28] The bulky tropane bicycle is bordered by Ser421, Phe319, Ala48, Asp46, Ala44 and Phe43. The DAT binding pocket is quite conserved and surrounded by mostly hydrophobic amino acid residues, demonstrating the need of an aliphatic backbone connecting a hydrogen bond acceptor group with aromatics. The inhibition of dopamine binding is achieved by the combined interactions of free amine, bulky tropane ring and aromatic phenyl ring hindering the conformational movements of DAT.[28] However, it is important to emphasize that all these interactions have been revealed as crystal structures of ligand-DAT complexes, where the role of the lipid-protein complex dynamics is not considered.

Mutagenesis studies have highlighted the amino acid residues Asp313 and Trp84 to be in or near the DAT binding pocket of cocaine and its analogue, β-CFT, since aspartate to asparagine and tryptophan to leucine mutations have increased the DAT's affinity for these ligands compared to wild-type. On the other hand, these mutations did not enhance, but decrease the binding affinity of piperazine-based inhibitors, e.g. GBR12909 (Scheme 2).[29,30] This suggests that tryptophan and aspartate are vital for GBR12909 analogues to retain strong

interactions with DAT, while Asp313 and Trp84 are somewhat inhibiting the interaction of tropane-based inhibitors.

DAT ligand types

Structures of various DAT ligands can be divided roughly into two main groups:

a) ligands that act either as substrates or partial allosteric modulators,
b) inhibitors.[21]

The former group consists of dopamine and structurally similar molecules (Scheme 1), which are potentially transportable ligands. The latter group is made up of inhibitors of various classes of compounds (Scheme 2), most potent are benzhydryl substituted piperazine derivatives (e.g. GBR12909 and GBR12935) and cocaine-like molecules (e.g. β-CPT).[21,31]

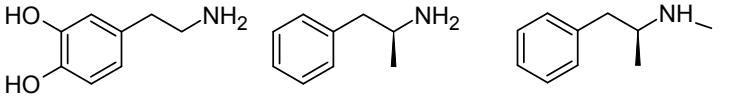

dopamine **(*d*)-amphetamine** **(*d*)-methamphetamine**

Scheme 1. Dopamine and other substrate-like DAT ligands.

A significant amount of literature focuses on piperazine-based compounds to find selective DAT inhibitors and it has been the second most probed scaffold besides tropane bicycle.[32–37] Among them GBR12909, also known as vanoxerine (Scheme 2), even entered clinical trials as a medication to treat psychostimulant, e.g. cocaine and methamphetamine, drug abuse but failed on its Phase I trials due to side-effect liabilities.[38,39] Some piperazine derivatives are also high affinity sigma receptor ligands, for example rimcazole is both DAT inhibitor and sigma-1 receptor antagonist.[40] It's thought that the dual interaction with DAT and σ receptors is a potential solution against psychostimulant addictions.[32,41] Among piperazine-based ligands the DAT affinity is usually not a problem, but the selectivity against other monoamine transporters and receptors is an issue.

A separate class of DAT inhibitors are benztropine analogues (Scheme 3a), while benztropine itself is used as an anticholinergic agent.[42] Benztropine and its *N*-substituted analogues have quite recently reported to be antagonists of cocaine and amphetamine self-administration.[43] The structure is similar to cocaine derivatives in that the tropane bicycle is the same, but benztropine has no substituent at the C-2 position and the C-3 substituent is in the *endo* or α-configuration (Scheme 3a). Benztropine and GBR-compounds share the same diphenylmethoxy moiety, which contributes to the different binding interactions

with DAT.[29] Numerous benztropine derivatives have been synthesized and their monoamine transporter affinities determined to yield several potent ligands.[44]

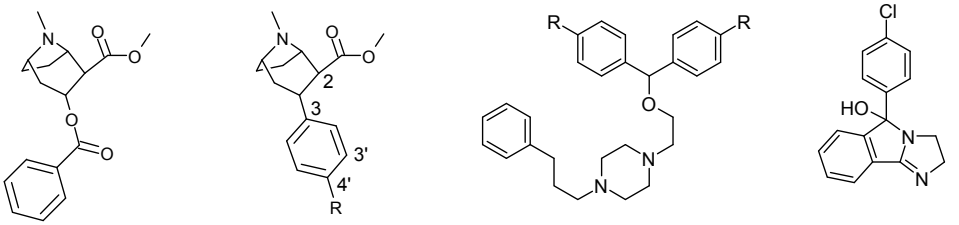

Scheme 2. Selection of DAT inhibitors.

Several other scaffolds for lead optimization of selective and potent DAT ligands have been proposed, e.g. trishomocubane,[45] substituted pyridines,[46] bivalent phenetylamines,[47] 4-hydroxy-1-methyl-4-(4-methylphenyl)-3-piperidyl 4-methylphenyl ketone,[48] 1-[1-(2-benzo[*b*]thienyl)cyclohexylpiperidine (BTCP)[49] and methylphenidate[50](Scheme 3b-g).

Polycarboxylic trishomocubane derivatives are σ receptor inhibitors, which had off-target affinity for other receptors in mammalian brain and their potential application for DAT imaging agent was investigated.[45] Wang and others focused on the geometrical positions and distances between nitrogen, carbonyl and phenyl ring of 3β-phenyltropanes to develop a new class of DAT inhibitors.[48] This approach did not yield ligands of even moderate monoamine transporter affinity. Enyedy et al. have more successfully managed the design of aryl-substituted pyridines as potent DAT ligands using similar technique of generating a new pharmacophore model from structural features of several classes of known DAT inhibitors.[46] Several pyridine-based DAT inhibitors with sub-nanomolar affinities and good selectivity were developed.[46] BTCP, an analogue of the abused drug phencyclidine, is known to be a dopamine uptake inhibitor and derivatives of BTCP have been developed to have moderate potency.[49,51] All of the aforementioned ligands are atypical dopamine transporter inhibitors and their derivatives have been thoroughly investigated, nevertheless their use has been quite scanty.

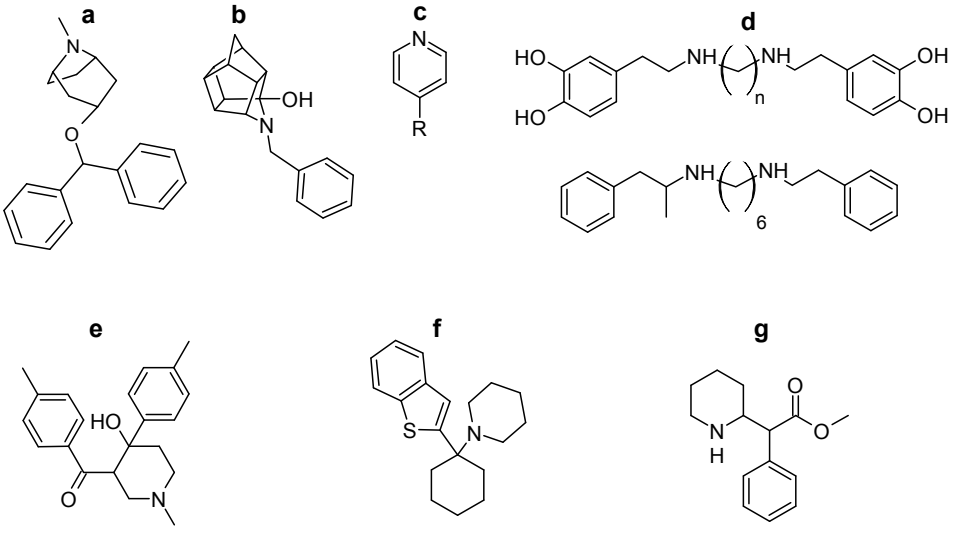

Scheme 3. Benztropine(a), trishomocubane (b), substituted pyridines (c), bivalent phenetylamines (d), 4-hydroxy-1-methyl-4-(4-methylphenyl)-3-piperidyl 4-methylphenyl ketone (e), 1-[1-(2-benzo[*b*]thienyl)cyclohexylpiperidine (f), methylphenidate (g) as DAT inhibitor scaffolds.

Tropane derivatives as DAT inhibitors

The extensive search for a potent monoamine transporter inhibitor among tropane derivatives, to find drugs for disorders connected with transporter, started in the 1970s with the identification of transporters as drug targets and intensified in 1990s with the cloning of transporter cDNA.[1] Several structural features determine the binding potency of cocaine-like ligands to DAT: stereo-chemistry and substituents at C-2, C-3 and *N*-positions of tropane core (Scheme 2).[52,53] Naturally (–)-cocaine, with substituents at C-2 and C-3 positions in the β-configuration (Scheme 2), has eight possible stereoisomers of which only (*R*)-(2β,3β)-cocaine is a potent psychostimulant.[29] Several reports confirm the sensitivity of DAT to the stereochemistry of the bicycle.[14,52,53] Therefore, synthesis starting from natural alkaloids allows to retain most of the stereocenters. One of the first modifications to yield tropane ligands with higher biological activity than cocaine, was the replacement of the benzoyloxy group by phenyl ring at the 3-position of cocaine (Scheme 2).[54,55] This replacement was the basis for the design of more potent DAT inhibitors. Modification of the [3.2.1]bicycle by elimination of the ethylene bridge of 3β-phenyl tropanes diminished its potency substancially.[54]

A significant correlation between potencies and self-administration exists among cocaine analogues, and therefore, self-administration can be predicted by DAT's affinity to compounds; this phenomena is absent among other monoamine transporters, e.g. NET and SERT.[56] The effect of substituents of tropane

derivatives to DAT potency and selectivity and some applications are discussed in the following paragraphs.

Introduction of reactive groups to potent DAT inhibitors allows to attach ligands to the protein binding pocket covalently. Azido-, isothiocyanate-and bromoacetate-based benztropine derivatives were developed as irreversible DAT inhibitors as potentially useful molecular probes.[57–59] An irreversible DAT ligand RTI-76 (3β-(*p*-chlorophenyl)tropan-2β-carboxylic acid p-isothiocyanato-phenylethyl ester) has been used to study the possibility of oligomeric assemblies among transporter proteins and rodent behavioral effects of blocking DAT to determine dopamine agonists and antagonists.[59,60]

The sensitivity of DAT to the C-2 position of tropane bicycle (Scheme 2) has been probed in several reports.[61–65] A set of fluoroalkyl esters and amides at the C-2 position of 3β-halophenyltropanes were tested against monoamine transporters to reveal that esters showed higher affinity than amides at both DAT and SERT. Even the tosylate esters had nanomolar affinities suggesting that SERT and DAT can tolerate bulky substituents at the C-2 position in β-configuration.[63] In order to increase the metabolic stability, the ester group at C-2 position of tropane ring has been replaced with substituted oxadiazol[61] and other heterocyclic[66] moieties and these modifications usually retained biological activity. This replacement also yielded ligands with slower onset of action and lower abuse liability than cocaine, and therefore, has been proposed as a substitute medication for treating cocaine abuse.[61] Even a series of dimeric tropane analogues, connected at position C-2 with different linkers, have been synthesized and their biological activity determined.[67] This analysis revealed that with an appropriate linker good DAT affinity could be achieved, but the binding to other monoamine transporters was also significant. Dimerization of high affinity ligand did not guarantee excellent binding of the dimeric compound.[67]

The DAT sensitivity to the C-3 position of tropane bicycle (Scheme 3) has been probed with bulky substituents at the 4'-position, revealing a remote binding cavity approximately two methylene groups from the 4'-position, on the DAT.[68] This cavity allows insertion of another aryl group to 4'-position when appropriate, e.g. (*E*)-olefinic, acetylenic or methyl acetylenic, linker is used.[68] Increase in potency, by addition of an extra aryl group, was not achieved, but the possibility to attach functional groups in order to improve any other property of the compound remains. The steric sensitivity of DAT to substituted 4'-phenyltropanes was studied also by Blough and others to find that substituents larger than ethyl group resulted in lower affinity for DAT and lower selectivity when compared to SERT.[69] From this, it can be concluded that phenyl, 4'-methylphenyl and 4'-halophenyl groups at 3β-position usually increase or retain DAT affinity, however, if large aromatic substituent is needed at 4'-position, a linker of at least few carbons would be necessary.

Combination of removal of *N*-methyl group with the addition of 4'-ethyl and 3'-iodo substituents led to a high affinity and selectivity for the SERT.[70] Replacement of *N*-methyl group with a functional group containing *N*-*N* bond

led to a significantly lower potencies compared to cocaine. This could be explained by the fact that decrease in electron density at the bridge nitrogen is responsible for the decrease in activity. This is not always the case since exchange of nitroso group with more electron withdrawing nitro group increases the potency more than tenfold. A discrepancy between dopamine uptake inhibition and binding affinities showed that some cocaine analogs were more active in the displacement experiments than in dopamine uptake inhibition, suggesting a possibility that these compounds are functional antagonists of cocaine.[71]

It has been suggested that from a steric point of view nortropane derivatives accommodate only small changes at the nitrogen position or on the aromatic ring at C-3.[53] Nevertheless, *N*-position of tropane bicycle has been probed by several reports.[71–73] The monoamine transporter affinities of *N*-substituted derivatives of β-CIT were analyzed and it was revealed that the basicity of tropane nitrogen was the only factor to determine DAT affinity if bulky and polar groups were introduced to the tropane nitrogen. It was concluded that even sterically large substituents are tolerated if the spacer is long enough.[72] Quaternization of cocaine and zwitterionic 2β-carboxylic acid cocaine derivative resulted in a loss of DAT bioactivity in a few orders of magnitude.[74]

Transition metal (Cr and Ru) complexes of 2β-carbomethoxy-3β-phenyl-tropane were synthesized in order to search potent ligands with spectrochemical ($Cr(CO)_3$) or radioactive (^{97}Ru) labels to probe biological systems.[75] The resultant Cr and Ru tropane complexes yielded low to moderate affinity ligands, which were rarely used afterwards.

The necessity of tropane nitrogen was tested by replacing it with oxygen or methylene bridge. This allowed designing of new compounds based on bicyclo[3.2.1]octane system, questioning the role of ionic bond of tropane nitrogen with hydrogen bond donor of the transporter.[76,77] Indeed, more than a few 8-oxabicyclo[3.2.1]octane and carbocyclic [3.2.1]octane derivatives showed at least as good affinity, and selectivity over SERT, as its nitrogen counterparts.[76,77] In addition, the configuration of C-2 and C-3 had also effect on the selectivity of DAT over SERT in these series and the absolute requirement of β-configuration of both carbons was contradicted, since many 2α and 3α non-nitrogen ligands were quite potent.[76,77] Nevertheless, β-configuration of carbons of tropane-based ligands at positions 2 and 3 in most cases yield more active DAT ligands than their α-analogues.

Reporter ligands

Numerous radiolabeled ligands have been used to study DAT *in vitro*. [^{3}H]Cocaine,[78] [^{3}H]β-CFT,[79,80] [^{3}H]β-CPT,[81] [^{3}H]Mazindol,[71] [^{3}H]GBR12935,[73] [^{125}I]β-CIT[82] and [^{3}H]PE2I[83] to name a few (Schemes 2–4). In addition, [^{3}H]dopamine has been used for uptake studies (Scheme 1).[84] Several tropane based PET and SPECT ligands have been developed to localize DAT in

mammalian brain including [^{11}C]PE2I,[85] [^{18}F]FE-PE2I,[86], [^{11}C] LBT-999,[87] [^{123}I]FP-CIT,[88] [^{18}]FP-CIT,[89] [^{123}I]-altropane[89] and [^{99m}Tc]TRODAT[89] (Scheme 4). Rhodamine (RTI-233) and 7-nitrobenzo-2-oxa-1,3-diazole labeled fluorescent monoamine transporter ligands have been developed, but were moderately affine (Scheme 5).[90,91] Fluoroprobes RTI-233, MFZ 9-18 and JHC 1-64 still have been used only very little to characterize amine transporters[92–94] when compared to reports using radioactivity labeled cocaine analogs. This could be explained by the relatively poor selectivity of these ligands for neurotransmitter transporters and by their moderate affinity.

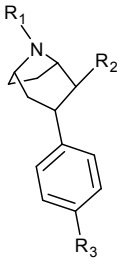

R_1 = CH_2CH=CHI, R_2 = CO_2CH_3, R_3 = CH_3	**PE2I**
R_1 = CH_2CH=CHI, R_2 = $CO_2CH_2CH_2F$, R_3 = CH_3	**FE-PE2I**
R_1 = CH_2CH=CHI, R_2 = CO_2CH_3, R_3 = F	**Altropane**
R_1 = CH_2CH=$CHCH_2F$, R_2 = CO_2CH_3, R_3 = CH_3	**LBT-999**
R_1 = $CH_2CH_2CH_2F$, R_2 = CO_2CH_3, R_3 = I	**FP-CIT**

Scheme 4. A selection of tropane-based ligands used for the localization of DAT *in vivo*.

Reporter ligands, used in *in vitro* displacement studies or in kinetic experiments, have to meet several criteria. These ligands must:

1) be specific for the target protein,
2) have high binding effectiveness,
3) form slowly dissociating complex, if slow separation methods are used to determine the bound ligand (e.g. filtration, centrifugation),
4) share the same binding sites with ligands under investigation,
5) carry sensitive labeling for determination of low concentrations,
6) be stable in the assay mixture during the analysis.

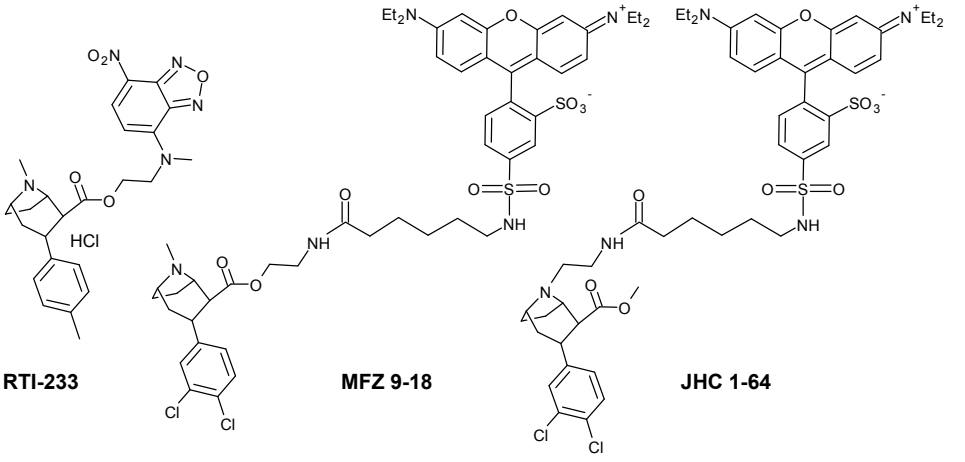

Scheme 5. Some tropane derivatives tagged with fluorescent labels.

Simulations of ligand binding kinetics

Ligand-receptor binding kinetics have been theoretically studied and kinetic curves have been simulated in a number of reports. [95–98] This theoretical approach would be unavoidable if experimental data reveal complex or uncommon binding kinetics. Here are some examples where simulations support experiments. The kinetics of chorionic gonadotropin binding to gonadotropin receptors were studied and binding time-curves were simulated since the kinetics appeared to be multiexponential.[95] This phenomenon was explained by the degradation of the binding hormone and receptor. A mathematical model, describing the simultaneous binding and degradation, was developed and simulated curves were computed. This approach allowed to estimate more correct rate constants and the extent of degradation.[95] Motulsky and Mahan derived a mathematical model, and solved it analytically, to simulate the kinetics of simultaneous binding of a ligand and its competitive inhibitor to a receptor. The effect of a slowly dissociating inhibitor, the length of reasonable incubation times and the determination of rate -and equilibrium constants from kinetic curves were discussed.[96] The effect of aggregation on the binding kinetics was analyzed in the case of insulin binding to insulin receptor.[97] Complex models, considering receptor aggregation and cooperativity, were constructed and the resulting differential equations were solved numerically to obtain computer simulations explaining kinetic data observed experimentally.[97] A situation, where a drug molecule can bind to a target protein in different orientations, was theoretically analyzed by Wittmann and Strasser.[98] The binding time-curves of labeled ligand competing with an unlabeled ligand capable of binding in two different orientations were simulated by solving a derived differential equation system numerically. Resulting kinetic curves of one- and two-orientation models were compared with experimental data to distinguish binding mode. Several ligand-protein systems, where one ligand exhibits a bivalent binding mode, have been reported.[99,100] The aforementioned cases use simulations of ligand-protein interactions to interpret uncommon experimental data in order to gain a more detailed insight about ligand or protein behavior. In all these cases, simulation of ligand-protein interactions was made to interpret uncommon experimental data and gain insight into ligand-protein interaction mechanism.

Kinetics of tropane derivatives interaction with DAT

Although, the inhibition constants of tropane derivatives have been determined extensively over the decades, kinetic characterization has not been a priority. The binding of [^{3}H]CFT (Scheme 2) to cocaine receptor (nowadays DAT) has been studied in 1989 and biexponential time course was found in both association and dissociation steps.[79] This was explained by two-component binding model with 4.7 and 66 nM dissociation constants, designated as high and low-affinity components, while the former component comprised about

90% of specific binding.[79] It was suggested that the low affinity component could be binding to other membrane proteins in sample tissue, e.g. other monoamine transporters. The low affinity binding site was later shown to be an artifact generated by freezing of caudate tissue.[101] The half-life of dissociation of [^{3}H]CFT was up to 100 times longer than reported for [^{3}H]cocaine, and also the non-specific binding of [^{3}H]CFT was almost two times less than that observed for [^{3}H]cocaine.[79] Due to slower dissociation rate, higher affinity and selectivity, compared to [^{3}H]cocaine, [^{3}H]CFT was considered, and extensively used today, as a radioligand probe for DAT.

Hasenhuetl et al. have used electrophysiological approach, i.e. whole-cell patch clamp system, to determine kinetic parameters of cocaine, methylphenidate and desipramine binding to DAT and SERT.[102] The observed rate of cocaine binding to hDAT was observed at multiple concentrations to yield k_{obs} versus concentrations graphs. Cocaine showed a linear dependence of the apparent rate constant upon ligand concentration, indicating a one-step binding mechanism.[102,103] The off-rate constant of cocaine-DAT complex was 0.35 s^{-1}, which is approximately two orders of magnitude faster than the off-rates of slowly dissociating ligands.[13,102]

The kinetics of several ligands, including GBR12909 (Scheme 2) and PE2I, to DAT have been studied before by Stepanov and Järv.[13,104] It has been shown that after initial binding of GBR12909 and PE2I to DAT an additional slow step of conformational isomerization of the complex occurred (Scheme 6). In addition, both ligands had very similar equilibrium and isomerization rate constants, and the contribution of the additional slow step increased the apparent affinities of both ligands approximately tenfold. This isomerization phenomena was not found in the case of dopamine and cocaine binding.[103]

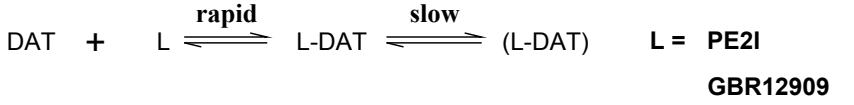

Scheme 6. Two-step binding mechanism of PE2I and GBR12909 to DAT.

N-(3-Iodoprop-(2*E*)-enyl)-2β-carbomethoxy-3β-(4'-methylphenyl)nortropane (PE2I) is a selective and potent ligand developed as a dopamine transporter inhibitor (Scheme 4).[73] PE2I is a DAT inhibitor with approximately 100 times greater potency than cocaine.[83] Therefore [^{11}C]-labeled PE2I has been one of the most used ligands to localize DAT in positron-emission tomography (PET) studies.[85,105] Since PE2I fulfills all prerequisites of a reporter ligand, it is used in this study to characterize other tropane-based ligands.

The inhibition constants acquired from displacement studies or dissociation constant derived from direct binding experiments reflect the overall dissociation constant of ligand-protein complex, yet these standardized experiments do not give information about the possible kinetic mechanism of ligand binding.

The overall inhibition constant (K_i or K_d) is related to the subsequent equilibrium constants (K_L and K_{isom}) (describing binding Scheme 6) by the following equation:

$$K_i = \frac{K_L K_{isom}}{K_{isom}+1} \quad (1)$$

Methods for the analysis of membrane protein-ligand interaction *in vitro*

Although, there are numerous methods to study the binding interactions between membrane proteins and ligands, only handful have been used to study ligand binding kinetics. Methods like isothermal titration calorimetry,[106] circular dichroism spectroscopy,[107] atomic force microscopy[108] and NMR[109] have been used to investigate some aspects of membrane protein-ligand binding, but have found little use when kinetic studies are in mind, due to several shortcomings inherent to those methods.

Radioactive ligand binding

Radioligand binding assay is the most versatile method so far to quantify equilibrium or kinetic parameters of membrane protein-ligand interactions. Although, being a relatively old method, it is still in use to validate any novel methods. The first kinetic evaluations started with the progress on radiolabeling techniques. In 1957 Wilzbach proposed a tritium-labeling method, where the compound of interest is exposed to tritium gas and the exchange of hydrogen to tritium occurs.[110] This method allowed preparation of [^{3}H]atropine to kinetically characterize the direct binding kinetics of atropine to acetylcholine receptor.[111]

The direct measurement of a radioligand kinetics is always more desirable, but in most cases a reasonable result can be obtained from indirect measurements. Several procedures exist to determine whether ligand forms a slowly dissociating stadium and to determine rate constants. “Infinite dilution” or isotopic dilution technique was proposed to measure the off-rate of radioligand from its complex with the target protein by a substantial dilution, this can be accompanied by the presence of an unlabeled compound.[112,113] The amount of bound radioligand is then determined at different time points after dilution. The dissociation of radioligand can also be initiated by the addition of concentrated unlabeled ligand with minimal dilution.[114] In many cases these techniques reveal different results and are often explained with radioligand rebinding after dilution.[114] Other option is to measure the apparent rate constants of radioligand association with increasing concentrations of unlabeled ligand.[14,115,116] This yields an observed rate versus concentration plots which could be solved to give rate constants of the slow step of ligand under investigation. There’s also a method by Motulsky and Mahan, where the rate constants of an inhibitor are determined by measuring

the effect of a single concentration of unlabeled inhibitor on the observed rate of the radioligand binding.[96,117] It should be noted that this procedure is adequate only in the simplest of competitive inhibition cases.

Surface plasmon resonance

A method where the receptor, or the ligand, is immobilized to a sensor surface under detergent-solubilized or lipid-reconstituted conditions and the minute changes in refractive index at the surface are measured.[118] For adequate results it is crucial that the protein retains its tertiary structure and activity in the substitute environment. The advantages of this method are small amount of material needed for a measurement, capability to detect fast complexes and being label-free.[118] On the other hand, the drawbacks include low-throughput, mass transport limitation, potential challenges in finding a strategy to attach the protein to a surface, while retaining the protein native function in an artificial lipid medium and sensitivity of detecting the interactions of small molecules is more difficult than of larger ones.[118,119] Nevertheless, SPR has been used to characterize kinetics of several membrane protein-ligand systems, including DAT[120] and D_3 dopamine receptor[121]. Based on SPR, handful of related methods have been developed, e.g. plasmonic-based electrochemical impedance microscopy (P-EIM)[122] and SPR microscopy[123].

Fluorescence-based methods

Several fluorescence based methods have been developed to study membrane protein-ligand interactions. Fluorescent labeled ligands can be used similarly as radioligands in determining equilibrium or kinetic constants of a ligand-protein system, where bound and free ligand are separated as in radioligand assays, e.g. filtration, chromatography, and quantified by fluorescence detector.[124] The only advantage of this method over radioligand binding would be the absence of radioactive waste from experiments. The sensitivity of fluorescence detection is typically lower than that of radioactivity, and issues with potential auto-fluorescence and change in ligand fluorescence emission due to environment are some drawbacks of this method.[124] A more advanced methods, e.g. based on ligand-receptor Förster resonance energy transfer[124] or fluorescence anisotropy,[125] has been used to study rapid binding kinetics. Försted resonance energy transfer based method needs covalent attachment of a fluorophore to both ligand and receptor and is based on the strong distance dependence of energy transfer between chromophores or fluorophores attached to the ligand and to the receptor.[124] It's important to emphasize that there is a possibility that the receptor function can be altered due to modification of the membrane protein structure and furthermore, if the fluorophore of a ligand is of comparable size with the ligand core structure, it would be difficult to study the effects of substituents of ligands since the largest effect would be caused by the fluorophore.

AIMS OF THE STUDY

The general aim of this dissertation was to investigate the kinetic mechanism of interaction of cocaine analogs with DAT and determine how this mechanism changes with ligand structure. This main goal was divided to the following objectives.

- Synthesis of a series of *N*-substituted nortropane derivatives for bioactivity measurements.
- Quantification of equilibrium and binding characteristics of interaction of DAT with the synthesized compounds.
- Comparison of shifts in inhibition and kinetic constants with changes in molecular structure to give insight about the interactions of DAT with other ligands within this bicyclic core structure.
- Derivation of a mathematical model to simulate binding time-curves of two simultaneously interacting ligands with a protein to specify differentiation between distinct mechanisms.
- Analysis of thermodynamic aspects of DAT thermal inactivation and estimation of the role of biomembrane in the stability and dynamic properties of transmembrane proteins.

EXPERIMENTAL

General methods

The buffer components were purchased from Lach-ner or Sigma-Aldrich. Whatman GF/B filters were used for the filtration assays. Fisher ScintiSafe 3 was used as a scintillation cocktail for counting of the samples. Radioactivity of the samples was measured with either Wallac 1219 Rackbeta or Wallac Guardian 1414 liquid scintillation counters. The binding data were analyzed using GraphPad Prism 4 software. Inhibition constants were calculated from IC_{50} values using Cheng-Prusoff equation[126], using 3 nM and 4.8 nM as the concentration of radioligand and the dissociation constant. *N*-(3-Iodoprop-(2*E*)-enyl)-2β-carbomethoxy-3β-(4'-methylphenyl)nortropane (PE2I) and its precursor were obtained from AS PharmaSynth and radiolabeled with [^{3}H]MeI as described before[115] yielding [^{3}H]PE2I with specific radioactivity of 69.4 Ci/mmol. The molar refractivities of compounds were calculated with ACD ChemSketch software. The purities of compounds were determined by HPLC (Agilent 1260–1290) analysis using a diode-array detector and Phenomenex Gemini-NX C18 column (5 μm, 4.6 mm × 250 mm), at wavelengths 220 and 254 nm. The purity was at least 95% at both wavelengths, except for compound **4j** which had purity slightly below 95% at 254 nm. Nevertheless, most of the compounds had purities above 99%. If conventional purification methods did not yield compounds with sufficient purity, additional purification was performed by preparative HPLC (Schimadzu) on a Phenomenex Luna C18 preparative column (5 μm, 15 mm × 250 mm) or flash chromatography (Biotage Isolera One) with a reversed-phase KP-C18-HS cartridge. Nuclear magnetic resonance spectra were recorded on a Bruker Avance III or Avance II spectrometer (700 or 200 MHz for ^{1}H and 176 or 50 MHz for ^{13}C), using tetramethylsilane (TMS) as internal standard. HRMS spectra were obtained using a Varian 910-FT-ICR mass spectrometer. Glassware used in air- and moisture-sensitive reactions was flame-dried or dried in an oven and then cooled under inert gas flow. Anhydrous solvents were distilled from CaH_2 or $LiAlH_4$ under an inert gas atmosphere.

Synthesis

Although, several synthesis strategies for a series of tropane derivatives exist,[127–129] starting from cocaine is by far the most common route. This path was firstly described by Clarke et al. and further investigated by many others.[54,55] The benefits of this approach would be the fixed configuration of natural alkaloid and extensive literature describing it. In short, the starting material (**1**, Scheme 7) was hydrolyzed and the resulting ecgonine was dehydrated with $POCl_3$. Subsequent anhydroecgonine was arylated with 4-methylphenylmagnesium bromide at temperatures below –40 °C and quenched at –78 °C by TFA yielding 2β-methoxy-3β-(4'-methylphenyl)tropane (**2**).[130] *N*-demethylation was

achieved by 2,2,2-trichloroethylchloroformate followed by Zn/AcOH. *N*-Alkylation of secondary amines with alkyl bromides with DiPEA as base in acetonitrile gave compounds **4a–4j**.[131] Alkylation of nortropane with tributylstannylprop-(2*E*)-ene chloride in ethanol and halogenation with NBS afforded compound **6**.

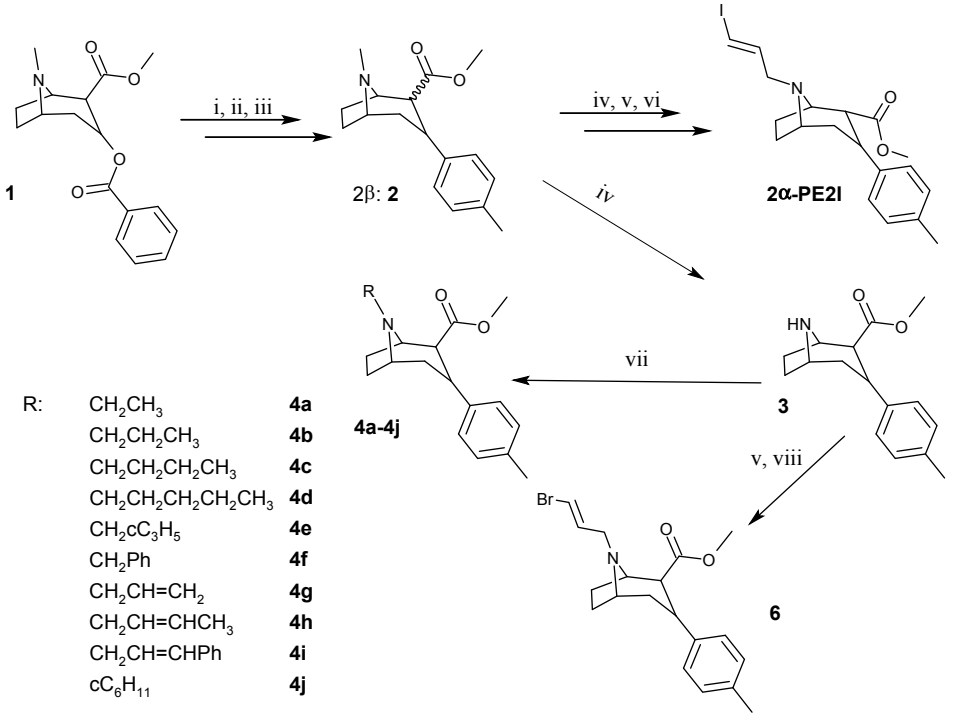

Scheme 7. General synthesis scheme of a series of *N*-substituted 2β-carbomethoxy-3β-(4'-methylphenyl)nortropanes. (i) HCl, reflux, 24 h; (ii) (a) $POCl_3$, reflux, 4–5 h, (b) MeOH, –45 °C 15 min, rt. 12 h; (iii) (a) *p*-tolylmagnesiumbromide, Et_2O, CH_2Cl_2, < –40 °C, 4 h, (b) TFA, –77 °C; (iv) Cl_3CCH_2OCOCl, reflux, 2 h, (b) Zn/AcOH, rt., overnight; (v) $Bu_3SnCH{=}CHCH_2Cl$, EtOH, TEA, KI, reflux, 2 h; (vi) I_2, $CHCl_3$, 0–2 °C, 4 h; (vii) RBr, DiPEA, MeCN, rt…reflux, 1…165 h; (viii) NBS, THF, rt., 1.5 h.

DAT

Membrane fragments of striata from adult C57BL/6 mice (mDAT) were used in DAT assay experiments. The striata were rapidly dissected, frozen and stored at –80 °C. The tissue was suspended in an ice-cold buffer (120 mM NaCl, 30 mM HEPES, 5 mM KCl, pH 7.4), sonicated with an ultrasound homogenizer (Bandelin SONOPULS) and centrifuged at 30,000 g at 0 °C for 15 min. The supernatant was discarded and the remaining pellet was resuspended in buffer and the process was repeated three more times to yield a membrane suspension that was divided into aliquots and stored at –80 °C until needed. The final membrane concentration was approximately 4 mg of wet tissue/ml.

Radioligand displacements

The membrane suspension of mDAT striatal fragments was preincubated with various concentrations of unlabeled ligand at 25 °C for 10 minutes before [^{3}H]PE2I, final concentration 3 nM, was added. After1 h of incubation, reaction was stopped by cold buffer and filtration. Filters were air-dried before transferring to scintillation vials. After addition of scintillation cocktail and shaking for approximately 12 h, the radioactivity was measured using a Wallac Guardian 1414 or Wallac Rackbeta 1219 liquid scintillation counter.

Kinetic experiments

Solution of a fixed concentration of [^{3}H]PE2I was added to a membrane suspension of mDAT to start the reaction at 25 °C. Aliquots were taken at different time points and the reaction was stopped with ice-cold buffer and filtration through GF/B filters. The kinetic curve was obtained after transferring filters to vials, addition of scintillation cocktail and measuring the radioactivity using liquid scintillation counter. CPM values were obtained using a Wallac Guardian 1414 or Wallac Rackbeta 1219 liquid scintillation counter. A more detailed procedure is reported in paper[14].

The effect of an unlabeled ligand to the reaction rate of [^{3}H]PE2I was conducted as follows. A solution of [^{3}H]PE2I (final concentration 3 nM) and various concentrations of unlabeled ligands were added to a membrane suspension of mDAT at 25 °C. The reaction was stopped and the kinetic curve was obtained as described above.[14]

Isomerization step

The binding mechanism of unlabeled ligand was analyzed by monitoring the influence of unlabeled ligand concentration on the observed rate constants (k_{obs}) of radioligand ([^{3}H]PE2I) binding with DAT. If the apparent rate of radioligand reaction increases, the pool of binding site decreases due to the isomerized complexes of both ligands, and therefore, the remaining protein is consumed faster. The apparent rate versus concentration of unlabeled ligand plot follows a hyperbolic dependence and the equilibrium binding constant (K_L) and rate constants (k_i, k_{-i}) can be obtained[104,132,133]:

$$k_{obs} = \frac{k_i^*[L^*]}{K_{L^*}^* + [L^*]} + \frac{k_i[L]}{K_L + [L]} + \frac{k_{-i}^* + k_{-i}}{2} \quad (2)$$

Similarly, if the observed rate constant, describing radioligand interaction with the binding sites in the presence of various concentrations of the unlabeled ligand, decreases, the equilibrium binding constant (K_L) of the unlabeled ligand could be calculated by the following equation[132,133]:

$$k_{obs} = \frac{k_i^*[L^*]}{(1+[L]/K_L)K_{L^*}^* + [L^*]} + k_{-i}^* \quad (3)$$

Simulation of protein-ligand interaction

A mathematical model describing simultaneous binding of two ligands (A and B) to protein (R) (Scheme 8) was constructed using principles of mass conservation and concepts of physical chemistry. Solving the subsequent ordinary differential equation system numerically allows simulating binding time-curves of the reporter ligand A.

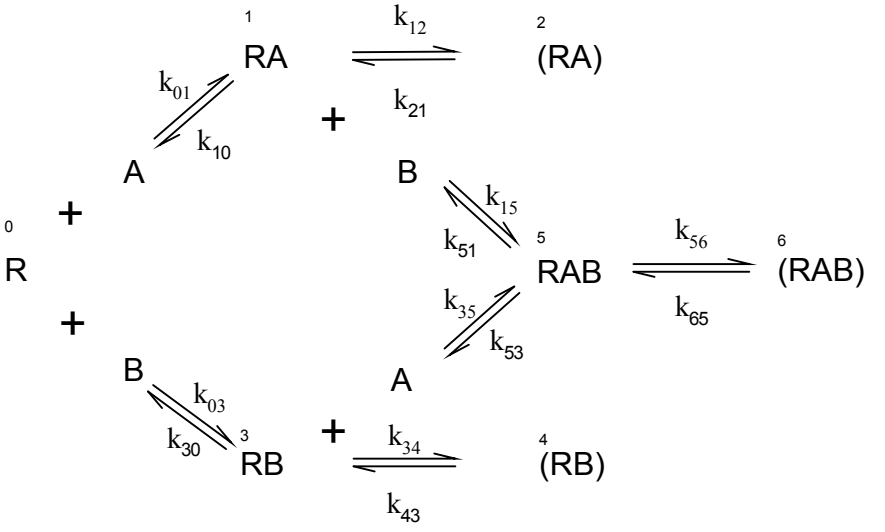

Scheme 8. General receptor (R), ligand (A) and ligand (B) interaction scheme.

Interactions, described in scheme 8, were presented by the following system of ordinary differential equations:

$$\frac{\mathrm{d[RA]}}{\mathrm{dt}} = k_{01}([\mathrm{A}]_{\mathrm{Tot}} - ([\mathrm{RA}] + [(\mathrm{RA})] + [\mathrm{RAB}] + [(\mathrm{RAB})]))([\mathrm{R}]_{\mathrm{Tot}} - ([\mathrm{RA}] + [\mathrm{RB}] + [(\mathrm{RA})] + [(\mathrm{RB})] + [\mathrm{RAB}] + [(\mathrm{RAB})])) + k_{21}[(\mathrm{RA})] + k_{51}[\mathrm{RAB}] - (k_{10} + k_{12})[\mathrm{RA}] - k_{15}[\mathrm{RA}]([\mathrm{B}]_{\mathrm{Tot}} - ([\mathrm{RB}] + [(\mathrm{RB})] + [\mathrm{RAB}] + [(\mathrm{RAB})]));$$

$$\frac{\mathrm{d[RB]}}{\mathrm{dt}} = k_{03}\big([\mathrm{B}]_{\mathrm{Tot}} - ([\mathrm{RB}] + [(\mathrm{RB})] + [\mathrm{RAB}] + [(\mathrm{RAB})])\big([\mathrm{R}]_{\mathrm{Tot}} - ([\mathrm{RA}] + [\mathrm{RB}] + [(\mathrm{RA})] + [(\mathrm{RB})] + [\mathrm{RAB}] + [(\mathrm{RAB})])\big) + k_{43}[(\mathrm{RB})] + k_{53}[\mathrm{RAB}] - (k_{30} + k_{34})[\mathrm{RB}] - k_{35}[\mathrm{RB}]([\mathrm{A}]_{\mathrm{Tot}} - ([\mathrm{RA}] + [(\mathrm{RA})] + [\mathrm{RAB}] + [(\mathrm{RAB})]));$$

$$\frac{\mathrm{d}[(\mathrm{RA})]}{\mathrm{dt}} = k_{12}[\mathrm{RA}] - k_{21}[(\mathrm{RA})];$$

$$\frac{\mathrm{d}[(\mathrm{RB})]}{\mathrm{dt}} = k_{34}[\mathrm{RB}] - k_{43}[(\mathrm{RB})];$$

$$\frac{\mathrm{d}[\mathrm{RAB}]}{\mathrm{dt}} = k_{15}[\mathrm{RA}]([\mathrm{B}]_{\mathrm{Tot}} - ([\mathrm{RB}] + [(\mathrm{RB})] + [\mathrm{RAB}] + [(\mathrm{RAB})]) + k_{35}[\mathrm{RB}]([\mathrm{A}]_{\mathrm{Tot}} - ([\mathrm{RA}] + [(\mathrm{RA})] + [\mathrm{RAB}] + [(\mathrm{RAB})])) + k_{65}[(\mathrm{RAB})] - (k_{51} + k_{53} + k_{56})[\mathrm{RAB}];$$

$$\frac{\mathrm{d}[(\mathrm{RAB})]}{\mathrm{dt}} = k_{56}[\mathrm{RAB}] - k_{65}[(\mathrm{RAB})],$$

where coefficients k_{ij} describe the corresponding rate constants, terms in square brackets are the molar concentrations of complexes depicted in Scheme 8. Formation of the complex (RA) was analyzed with a sum of two exponents to yield the specific binding (a) and reaction rate coefficients (b):

$$[(\mathrm{RA})] = -a \cdot \exp^{-bt} - c \cdot \exp^{-dt} \quad (4)$$

MATLAB version 9.1.0 with Curve-Fitting Toolbox (2016b, Mathworks, USA) was used for the simulations. The ordinary differential equation system was solved numerically with the MATLAB ode23s function designed to solve stiff differential equations. The simulated [(RA)] formation time curves were fitted with the MATLAB fit function with option exp2 (Equation 4).[134]

RESULTS AND DISCUSSION

Kinetics of DAT thermal inactivation

The knowledge of speed of spontaneous loss of binding sites is vital when designing experiments, where longer incubation times of reaction mixture with protein samples are needed. Therefore, thermal inactivation kinetics of DAT was studied by quantifying the specific binding of a selective DAT radioligand [^{3}H]PE2I over time. The time-course of spontaneous loss of DAT binding sites was monitored at different temperatures (Figure 2). This inactivation kinetics was not changed in the presence of protease inhibitor cocktail (Roche), confirming the fact that the observed process was not caused by proteolytic action of enzymes.

The decay of specific binding was monitored at 0, 12, 25 and 37 °C, and it was found that the thermal inactivation was described by exponential function:

$$B_t = B_{ns} + B_\infty exp(-k_{inact}t) \quad (5)$$

where B_t is the observed radioligand binding at time moment t, B_{ns} is the non-specific radioligand binding, B_∞ is the maximum specific binding and k_{inact} is the DAT inactivation rate constant. Specific binding at time t was calculated as $B_{sp} = B_t - B_{ns}$. The inactivation rate constants were calculated by using Eq. 5. Summary of the results obtained for rodent DAT are presented in Table 1.

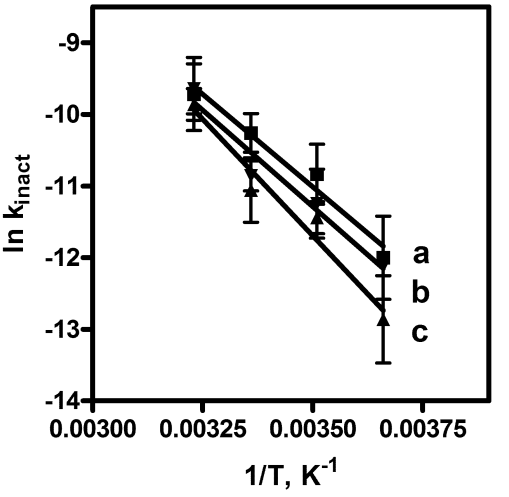

Figure 2. Arrhenius plots of thermal inactivation of mDAT (a), rDAT (b) from striatal membranes and rDAT (c) from PC-6.3 cell membranes.

DAT is not very stable in the form of a membrane suspension at 25 °C and above. Therefore, the incubation times used for binding studies and kinetic experiments should be chosen so that the loss of active sites through inactivation process remains negligible. In this thesis, the kinetic experiments were performed at 25 °C with timeframe in the order of ten minutes, whereas the half-life of loss of mDAT binding sites at the same temperature is approximately 330 min. This indicates that the contribution of thermal inactivation during kinetic experiments is negligible.

Table 1 Rate constants of thermal inactivation of dopamine transporters from brain striatal and cell membranes. Data from paper **I**.

Temperature	$k_{inact} \cdot 10^3$, min^{-1}		
	mDAT	rDAT	rDAT (PC-6.3 cell-line)
0˚C	0.26 ± 0.05	0.37 ± 0.05	0.33 ± 0.08
12˚C	0.76 ± 0.05	0.97± 0.09	0.80 ± 0.1
25˚C	2.1 ± 0.5	2.1 ± 0.1	1.2 ± 0.1
37˚C	3.0 ± 0.2	3.7 ± 0.3	3.9 ± 0.6

Comparison of thermal inactivation of DAT with stability of other proteins

In order to position the DAT stability among the stability of other proteins, the activation energies of thermal inactivation of other membrane and soluble proteins were compiled from the literature.[135–148] It was found that the activation energy of protein denaturation depends on the size of the protein molecule, and this dependence can be illustrated in the activation energy (E_a) versus molecular weight (MW) plot (Figure 3). This plot includes data for single subunit soluble and transmembrane proteins. It can be seen that soluble and membrane proteins behave very differently, and data for DAT inactivation agree with the latter group of proteins.

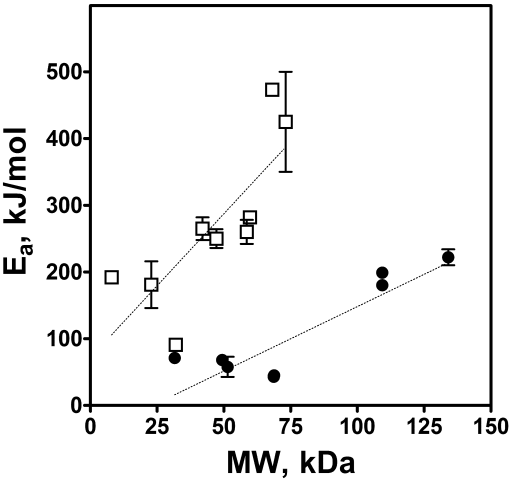

Figure 3. Comparison of activation energy of thermal inactivation of soluble (□) and membrane (●) proteins. Soluble proteins: G-actin,[135] stem bromelain,[136] carboxypeptidase A,[137] thermolysin,[138] RTX-8,[139] Cry3 δ-endotoxin,[140] lipase 1,[141] acetylcholinesterase[142] and peroxidase[143]; transmembrane proteins: hDVAC-2,[144] muscarinic receptor M1,[145] dopamine D1 receptor,[146] mDAT, rDAT from rat striatum, rDAT from PC-6.3 cell line, Ca^{2+}-ATPase from myosin and actomyosin,[147] human Ca^{2+}-ATPase[148].

Simulation of protein-ligand interaction kinetics

To establish how unlabeled ligands affect the kinetics of interaction of a labeled compound with a protein, a series of simulations were undertaken. This was accomplished by deriving a mathematical model describing the interactions of two ligands with a receptor (Scheme 8), solving the derived ordinary differential equation system numerically, and by calculating the specific binding time curves of reporter ligand A and receptor R complex formation. For similarity with experimental radioligand binding assay, formation of the isomerized complex (RA) was simulated, as this complex is determined by using slow methods (e.g. filtration) to separate the bound from unbound radioligand. This mathematical model allows simulation of kinetic behavior of interaction of two competing ligands binding in different mechanisms, therefore, providing an oppurtunity to distinguish slowly dissociating complex and possibly inhibition mode. For this analysis, the dependencies of ligand concentrations on the specific binding and the observed rate constant of the reporter ligand interaction with the binding site should be determined. By contrasting these plots, the two reaction schemes can be differentiated.

Firstly, if ligand B forms only rapidly dissociating complex with receptor R (Scheme 9), the observed rate and specific binding of reporter ligand A binding to R decreases with increasing concentrations of B (Figures 4a and 5a).

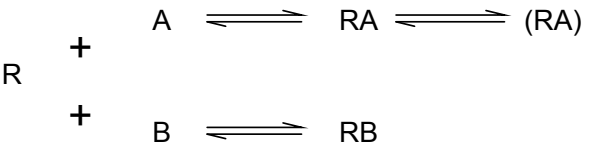

Scheme 9. Competitive binding of reporter ligand A and ligand B. B forms only rapidly dissociating complex RB.

Decrease in specific binding of A with increasing B concentrations is expected when ligands competitively inhibit the binding of each other and this effect can always be overcome by addition of A, as seen in Figure 4a. Similarly, the observed reaction rate decreases with increasing B concentration and this can also be overcome with sufficiently high A concentration (Figure 5a).

Scheme 10. Competitive binding of reporter ligand A and ligand B. After initial binding B forms an isomerized complex (RB).

Secondly, if both ligands A and B initiate isomerization step (Scheme 10), a decrease of specific binding with increasing concentration of competitive ligand B is expected (Figure 4b), similarly as in Figure 4a. However, the observed rate of reporter ligand A binding increases with increasing presence of ligand B (Figure 5b). This completely different trend is a clear indicator of reaction mechanism, illustrated in Scheme 10 and it's caused by faster depletion of the receptor to a stable unlabeled ligand-receptor isomerized complex with an unlabeled ligand.

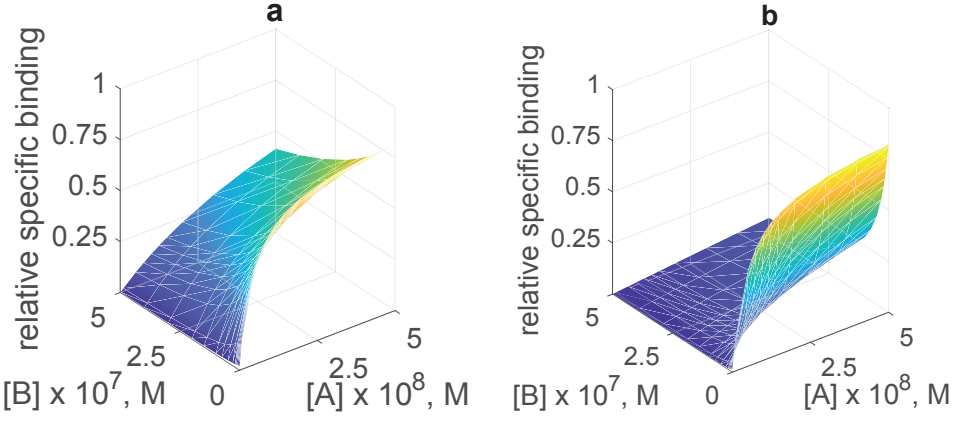

Figure 4. The effects of concentrations of competitive ligands A and B to the relative specific binding of ligand A: ligand B forms only rapid complexes with R (a); ligand B is capable of forming an additional slow step (b).

The possibility of kinetic differentiation between these two mechanisms is illustrated by simulation results. A more thorough analysis of kinetic models is described in paper **III**.

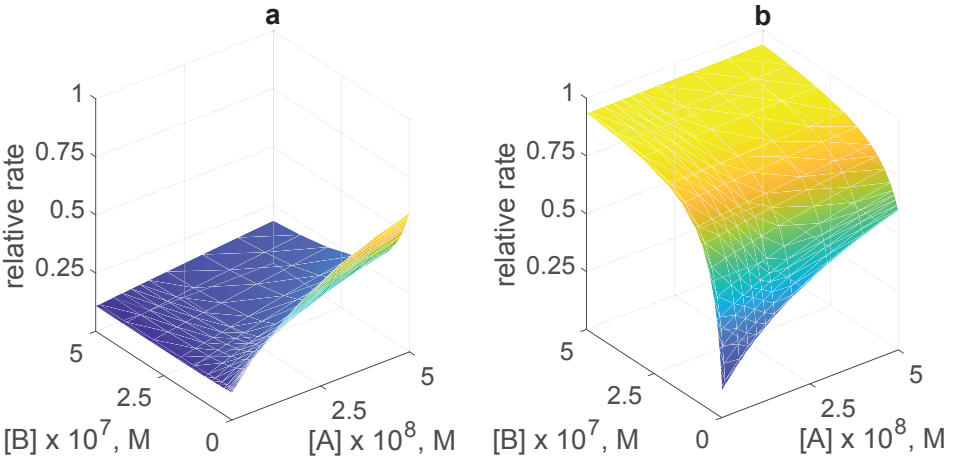

Figure 5. The effects of concentrations of competitive ligands A and B to the relative observed rate of binding ligand A binding to receptor R: ligand B forms only rapid complexes with R (a); ligand B is capable of forming an additional slow step (b).

Characterization of ligands

The synthesized ligands were characterized by measuring the DAT interaction constants, i.e. inhibition constant (K_i), initial equilibrium dissociation constant (K_L), on- and off-rate constants (k_i, k_{-i}) of the isomerization step. These constants were determined relative to the radioligand [^{3}H]PE2I. The inhibition constant values were calculated from IC_{50} values, derived from standard displacement experiments. All ligands, discussed here, completely inhibited the radioligand binding to DAT, revealing a typical single sigmoid and, therefore, indicating to a single binding site. The plateaus of kinetic curves also represented data points in inhibition curve and coincided with displacement studies, confirming that the kinetic curve indeed reached a plateau.

Effect of ligand structure to DAT affinity

DAT inhibition constants of *N*-substituted 2β-carbomethoxy-3β-(4'-methyl-phenyl)-nortropanes varied in the range of 2.9 to 321 nM (Tables 2 and 3), which is roughly two orders of magnitude. Sterically bulky cyclohexyl (**4j**) derivative was not tolerated by the binding site, but larger benzyl (**4f**) and cinnamyl (**4i**) groups were much more potent. These substituents have one and three carbon atoms connecting the phenyl and amine groups. This increases flexibility of the substituent and possibility for aromatic-aromatic interactions.

Table 2 DAT binding affinities (K_i) and equilibrium binding constants (K_L) of *N*-substituted 2β-carbomethoxy-3β-(4'-methylphenyl)nortropanes. Data from papers **II** and **IV**.

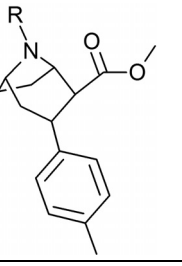

Compound	R	K_i ± SEM, nM	K_L ± SEM, nM
3	H	19 ± 3	26 ± 10
4e	$CH_2cC_3H_5$	36 ± 4	30 ± 7
4f	CH_2Ph	33 ± 6	56 ± 23
4g	$CH_2CH{=}CH_2$	65 ± 13	96 ± 44
4h	$CH_2CH{=}CHCH_3$	53 ± 6	53 ± 18
4j	cC_6H_5	321 ± 43	474 ± 160
2α-PE2I	$CH_2CH{=}CHI$	$(39 \pm 8) \cdot 10^3$	$(58 \pm 23) \cdot 10^3$

Homological series of *N*-alkyl nortropane derivatives (**3**, **2**, **4a–4d**) showed no clear dependence between number of carbon atoms and DAT potency, i.e. there seems to be no correlation between substituent size and protein affinity among linear alkyl chains. Within this series, increase of carbon chain length from methyl (**2**) to propyl (**4b**) leads to a decrease in potency of compounds, but further increase of length, up to *n*-pentyl (**4d**), increases DAT affinity. An arbitrary explanation could be the change in orientation of the ligand in the binding pocket or increase of hydrophobic interactions.

N-allylic substituents reveal a clear correlation between DAT affinity and substituent size, in the order of potency: cinnamyl (**4i**) > iodoallyl (**PE2I**) > bromoallyl (**6**) > crotyl (**4h**) > allyl (**4g**). This tendency implies that a somewhat rigid three carbon structural fragment in the ligand structure is needed if large substituents are desired at *N*-position of nortropane core. In addition, it seems that the phenyl group and halogens of allyl derivatives contribute by gain of interactions with the binding site.

The inhibition constant values of compounds **2** and **3**, in addition to thoroughly characterized PE2I, have previously been reported, revealing variable results. In theory, the K_i values should be independent of experimental conditions. The DAT affinity (K_i) of **2** in the literature varies between 1.5 and 32 nM, which agree with inhibition constant determined here (Table 3).[149,150] Similarly to compound **2**, the potency of **3** is also overestimated in the literature[149] with DAT affinity of 0.8 nM compared to 19 nM (Table 2). The inhibition constant, determined in this work, of PE2I agrees with a previous report[13] but slightly differs from 17 nM reported before[73]. The fact that different inhibition constant values are published for the same compounds is a common problem in the literature, and hinders constructing large structure-activity relationships.

Table 3 DAT binding affinities (K_i), equilibrium binding constants (K_L) and rate constants of isomerization of *N*-substituted 2β-carbomethoxy-3β-(4'-methylphenyl)nortropanes. Data from papers **II** and **IV**.

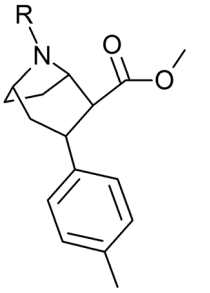

Compd	R	K_i ± SEM, nM	k_i, s^{-1}	k_{-i}, s^{-1}	K_L ± SEM, nM	K_{isom}
2	CH_3	5.7 ± 0.7	0.055 ± 0.002	–	11 ± 2	1.08
4a	CH_2CH_3	14 ± 2	0.035 ± 0.020	–	21 ± 2	2.00
4b	$(CH_2)_2CH_3$	32 ± 3	0.037 ± 0.002	–	65 ± 19	0.97
4c	$(CH_2)_3CH_3$	20 ± 2	0.05 ± 0.02	–	47 ± 11	0.74
4d	$(CH_2)_4CH_3$	9.6 ± 1.1	0.012 ± 0.001	0.0042 ± 0.0005	36 ± 9	0.36
4i	$CH_2CH{=}CHPh$	2.9 ± 0.3	0.036 ± 0.006	0.0048 ± 0.0001	41 ± 9	0.08
6	$CH_2CH{=}CHBr$	6.8 ± 1.1	0.005 ± 0.001	0.0046 ± 0.0003	23 ± 9	0.42
PE2I	$CH_2CH{=}CHI$	4.8 ± 1.0	0.020 ± 0.008	0.0024 ± 0.0003	37 ± 24	0.15

It is clear that the *N*-substituent alters the inhibition constant values of nortropane derivatives. Several substituted derivatives had increased potencies over the *N*-unsubstituted nortropane (**2**), revealing an enhancement of interactions between substituted ligand and the protein.

Kinetic profiles of ligand-DAT interaction

The dissimilarities of K_i and K_L are evident among ligands capable of inducing the isomerization step (Table 3). Splitting overall affinity (K_i) into initial binding (K_L) and isomerization (K_{isom}) constants can only be achieved by the analysis of their kinetic profiles. The on-rate constants of the isomerization process varied from 0.005 to 0.055 s^{-1} and revealed no correlation between ligand size and k_i. The off-rate constants (k_{-i}) are rather similar to one another, ranging from 0.0024 to 0.0048 s^{-1} (Table 3).

The kinetic profiles, in this case the observed rate (k_{obs}) of reporter ligand binding versus concentration of unlabeled ligand plots, between the ligands analyzed here are shown in Figures 6 and 7. It can be seen, that in many cases the presence of the non-radioactive ligand increased the observed rate, pointing to the fact that additional slow isomerization step follows the fast initial ligand binding step (Scheme 10). In the case of other ligands, decrease in the k_{obs} values can be seen in the presence of unlabeled ligands, pointing to the fact that

no isomerization of the complex was observed in their interaction with DAT (Scheme 9).

Similarly to inhibition constant, the ability to form a slowly dissociating complex does not directly correlate with *N*-substituent size among the data discussed here. In case of smaller homological subsets, e.g. *N*-allyl or linear *N*-alkyl, there seems to be a relationship between ligand volume and the presence of isomerization step. For example, *N*-allyl- (**4g**) and *N*-crotyl- (**4h**) substituted ligands (Table 1) exhibit only fast kinetics, while larger iodo- (**PE2I**), bromo- (**6**) and phenylallyl (**4i**) derivatives show a slow step with increasing on-rate constant of the slow step (k_i) with increasing size. Benzyl (**4f**), cyclohexyl (**4j**) and methyl cyclopropyl (**4e**) derivatives revealed only rapid kinetics (Table 2, Figures 6 and 7).

In the homological *N*-alkyl series of 2β-carbomethoxy-3β-(4'-methyl-phenyl)-nortropanes both fast and slow kinetics can be seen. Nortropane (**3**) displayed only rapid complex, while *N*-pentyl derivative (**4d**) showed a clear isomerization step. *N*-methyl (**2**), ethyl (**4a**), propyl (**4b**) and butyl (**4c**) substituted nortropanes revealed an isomerization step, which was interfered by high concentrations of the same ligand. This non-hyperbolic kinetics was observed among four ligands (**2**, **4a**, **4b** and **4c** in Figure 6) studied here. A decrease in the observed rate constant at relatively high concentrations of the unlabeled ligand could be caused by phenomenon, that is analogues to substrate inhibition, common in enzyme kinetics[151]. These non-hyperbolic curves are the results of two to one stoichiometry between ligand and protein. If this is the case, DAT can accommodate a second ligand with affinities five to tenfold less potent than the primary binding site.

The difference between overall affinity (K_i) and initial binding equilibrium (K_L) is somewhat expressed by K_{isom}, i.e. equilibrium constant describing the extent of isomerization of the ligand-DAT complex. Ligands, showing only fast kinetics, have similar or indistinguishable K_i and K_L values and, therefore, the isomerization phenomena is absent or insignificant.

The ligands, binding only in rapid complexes, show a declining plateau at approximately 0.022 s^{-1} when extrapolating the hyperbola. This limit is set by the isomerization rate constants of the radioligand, [^{3}H]PE2I. The upper plateau of ligands, exhibiting slow isomerization step (e.g. **4d**, **4i** and **6**), is directly related to their on-rate constants. The plateau is higher with increasing on-rate constants of unlabeled ligands.

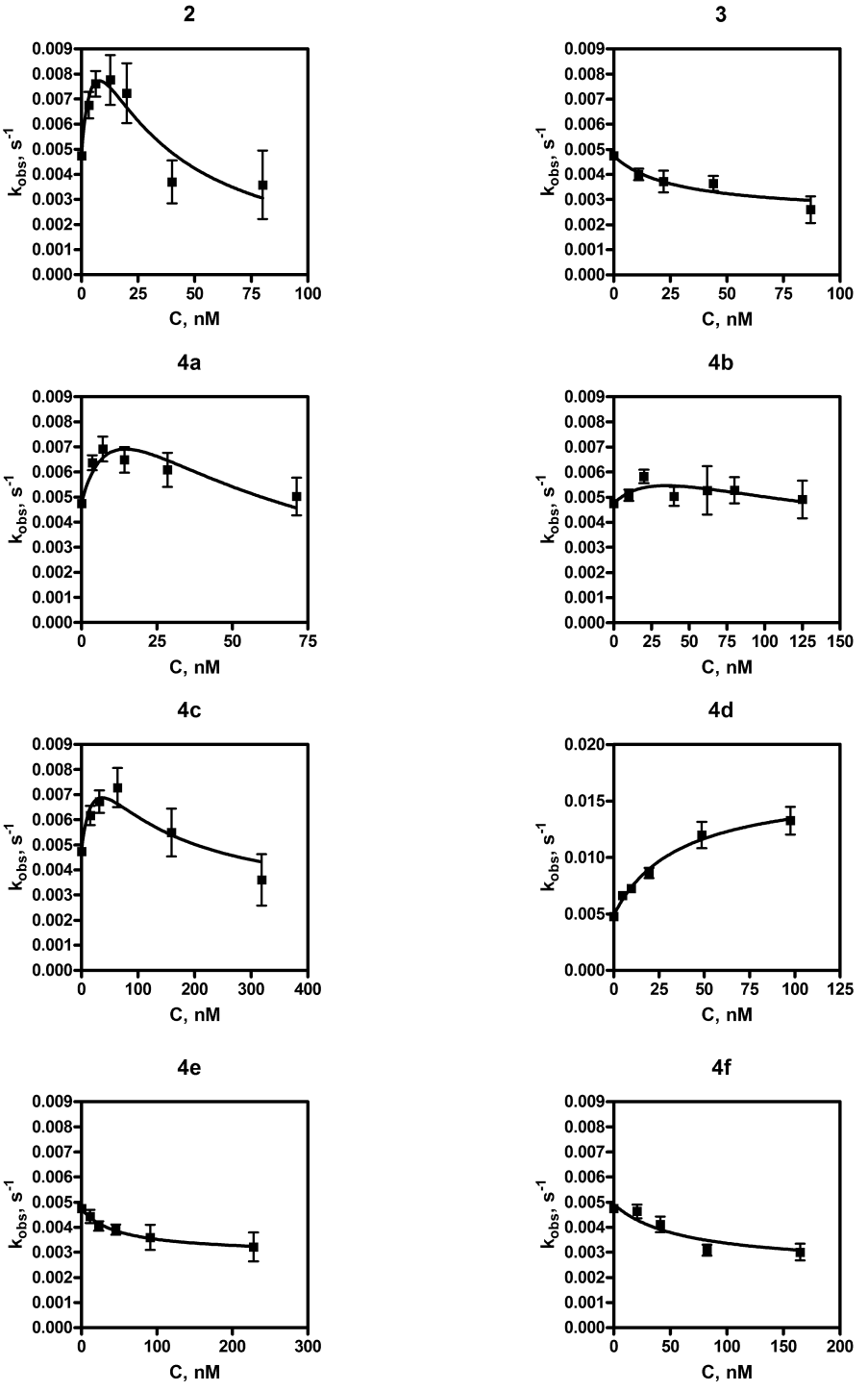

Figure 6. The effects of concentrations of compounds **2**, **3** and **4a-4f** on the observed rate constant.

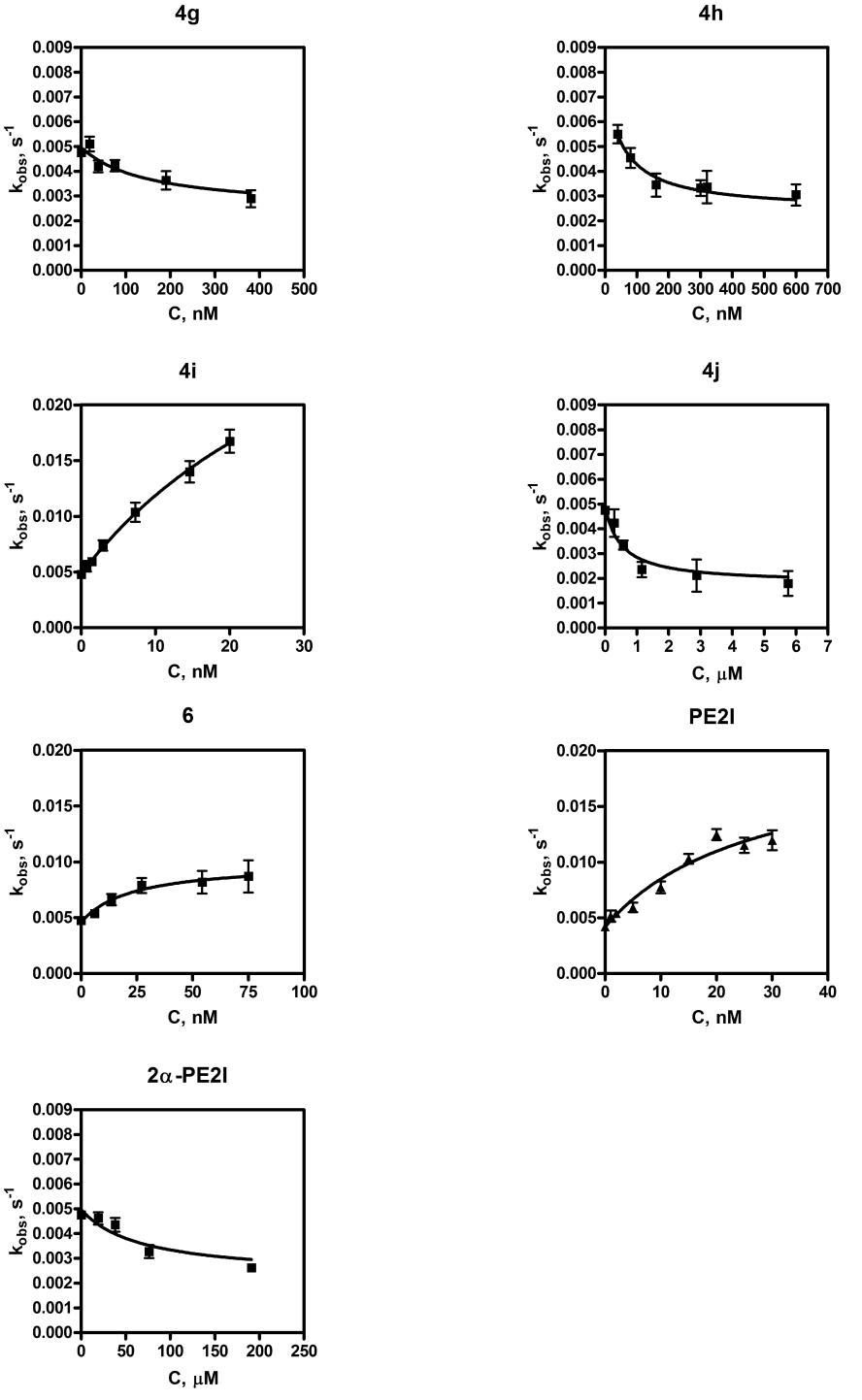

Figure 7. The effects of concentrations of compounds **4g-4j**, **PE2I** and **2α-PE2I** on the observed rate constant.

The role of ligand size to binding mechanism

Systematic structure-activity analysis was not an objective of this study, but still the data indicated some trends connected with ligand structure. The influence of molecule size, represented by molar refractivity (MR), to the dissociation constants was analyzed and the resulting trends are briefly summarized below.

In order to analyze the effect of the size of compounds on ligand-protein interaction, MR is correlated with the equilibrium binding and isomerization constants. The negative logarithm of the first equilibrium binding constants (pK_L) versus MR plot reveals a slight declining trend between them (Figure 8a), i.e. increase in *N*-substituent size results in a small decline of initial complex formation. This indicates that the first step of DAT interaction depends little on ligand size and larger ligands might have a slight steric hindrance upon initial binding. The same tendency seems to govern both ligand types with isomerization step and those without it. The first step of interaction is the molecular recognition of the compound by the protein. This tendency is not surprising since the diffusion of smaller molecules to the binding pocket is less restricted than that of a large molecule.

In order to explain high DAT affinity for some large ligands, considering declining K_L, an overall increase in affinity from isomerization component is needed. Ligands exhibiting isomerization step retain their potency by the increased contribution of the second binding equilibria, characterized by K_{isom}. It can be seen that the equilibrium is shifted towards slowly dissociating complex with increasing ligand size (Figure 8b), showing that the only option to retain DAT potency for a large ligand involves extending the isomerization step.

Molar refractivity was chosen in this case to represent the size of the molecule, and therefore, assess the shifts of equilibrium constants with increasing size, resulting in the simplest of structure-activity and structure-kinetics relationships. This study could be extended by the addition of more complex models and further modification of ligand structure to yield additional kinetic and equilibrium constants followed by a more thorough analysis of structural characteristics leading to those properties. Since the factors governing off-rate kinetics of any ligand-protein system are only very vaguely understood, the structure-kinetics relationships could be an invaluable asset to screening of compounds with desirable kinetics.

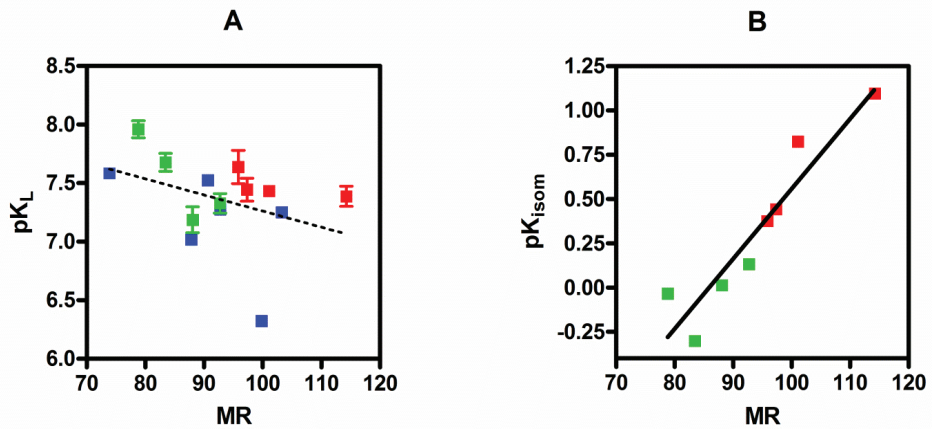

Figure 8. The effect of ligand size on the subsequent binding constants; ligands exhibiting only rapid kinetics (blue), ligands capable of initiating isomerization step (red), ligands capable of forming an isomerization step and a second rapid complex at high concentrations (green).

CONCLUSIONS

Cocaine analogues interact with DAT in two distinct mechanisms, which differ from one another by the presence or absence of a slow isomerization step. These interaction mechanisms can be differentiated by means of kinetic analysis, while common displacement studies do not allow this differentiation. Therefore, the results of this study provide unique opportunity to analyze the influence of ligand structure on the mechanism of their interaction with DAT, including their ability to induce a slow isomerization step.

Among the inhibitors analyzed here, all ligands with DAT affinities in the order of 10 nM or below initiated a slow isomerization step. This means that the overall gain in DAT affinity is contributed by the slow isomerization step and allows to speculate that all tropane-based high affinity DAT inhibitors owe their binding effectiveness to the slow step. Other ligands, with DAT affinities characterized by higher K_i values, ranging up to 321 nM in this study, did not initiate the slow isomerization step.

Contribution of the isomerization step increased with ligand size and the largest ligand displayed the highest potency. This means that the isomerization step is sensitive to ligand structure, similarly with ligand recognition in the fast binding step. Gaining knowledge about the slow isomerization step and how this step is influenced by structure may be useful for the design of drugs with increased binding effectiveness. This also means that all structure-activity relationships only based on K_i values, without any further verification of kinetic mechanism of binding process, may provide inadequate models.

In some cases, the isomerization process was inhibited by the ligand excess that is analogous with substrate inhibition phenomenon in enzyme kinetics, pointing to the possibility of formation of additional complexes in DAT inhibition.

The activation energy of thermal inactivation shows a positive linear correlation between protein molecular weight and activation energy. The thermal inactivation energy of membrane protein is lower than that of a soluble protein of similar size, therefore, the membrane is responsible for the lower activation energy. This is also a reminder that protein solubilization or proteins expressed in non-mammalian cells can alter the function and bioactivity.

SUMMARY

A series of *N*-substituted 2β-carbomethoxy-3β-(4'-methylphenyl)nortropanes were synthesized and their interactions with rodent dopamine transporter were studied. In addition to conventional equilibrium displacement studies, kinetics of interaction of these ligands to DAT was assayed, which allowed to further specify the ligand-protein interaction mechanism. It was found that several congeners were able to induce an additional slow conformational transition of the ligand-protein complex that increases the apparent DAT affinity. Among these ligands were some which deviated from the simple competitive models by displaying non-hyperbolic kinetics. This phenomenon, occurring at high concentrations, is not yet fully understood and needs further analysis.

The kinetic experiments were performed by monitoring the effect of unlabeled ligands to the binding kinetics of a single radiolabeled ligand [^{3}H]PE2I to DAT. In order to fully comprehend this kinetic approach, a general reaction scheme was compiled, ordinary differential equation system was constructed and solved numerically to yield simulated binding curves. Results of these simulations were used to formulate kinetic tools for differentiation between distinct ligand interaction mechanisms and identifying compounds capable of forming slowly dissociating complexes.

Characterization of fast and slow steps in the overall ligand binding process, and distinction between compounds, which are able and which are not able to induce the slow conformational transition of the transporter protein, opens an opportunity to analyze molecular recognition of these ligands by DAT. All ligands with apparent affinity around or below 10 nM were capable of inducing a slow conformational transition of protein-ligand complex, indicating the necessity of this property for efficient drugs. It can be proposed that all tropane-based high affinity DAT ligands owe their binding effectiveness to the slow step, and therefore, by increasing the contribution of the isomerization step, even more potent inhibitors could be designed. Although the proof of principle was illustrated in the case of tropane derivatives binding to DAT, modulation of overall binding effectiveness by an additional slow step could be used for other ligand-protein systems.

Only by modifying substituents at the nitrogen position of nortropane, the affinity of compounds changed from 3 to 321 nM. This variation was also sufficient to modify the ligand binding mechanism. *N*-Allyl derivatives showed a positive correlation between substituent size and DAT affinity, indicating the need of a moderately rigid chain of at least three carbons between the N atom of tropane bicycle and a bulky substituent. This allows retaining or even increasing transporters affinity for tropane-based ligands with increasing molecular weight.

Thermal stability of mouse and rat dopamine transporters was determined by measuring the loss of activity at a range of temperatures. Arrhenius equation allowed calculation of activation energy and half-lives of thermal inactivation. The activation energy values were compared to other soluble and membrane

proteins which showed an increase in activation energy with increasing molecular weight. Membrane proteins were significantly more labile than soluble proteins of similar size. Results of this study conformed the understanding about the significant role of lipid environment on DAT stability, and perhaps also on its kinetic behavior in the ligand binding process.

SUMMARY IN ESTONIAN

N-Asendatud nortropaani derivaatide kineetilised aspektid seondumisel dopamiini transportvalguga

Käesoleva töö käigus sünteesiti seeria *N*-asendatud nortropaani derivaate ning määrati nende tasakaalulised ja kineetilised konstandid seondumisel dopamiini transportvalguga (DAT). See võimaldas täpsustada ligandide seondumise mehhanismi, mille tulemusena tuvastati mitmed ühendid, mis olid võimelised moodustama aeglaselt dissotsieeruva ligand-valk kompleksi ning seeläbi suurendasid valgu näivat afiinsust ligandi suhtes. Tasakaalu tingimustes tehtud katsetes neid mehhanismi eripärasid tuvastada ei ole võimalik.

Kineetilistes mõõtmistes kasutati triitiumiga märgistatud reporterligandi [^{3}H]PE2I (*N*-(3-iodoprop-2*E*-enüül)-2β-karbometoksü-3β-(4'-metüülfenüül)-nortropaan) ning uuriti selle ligandi DAT-ile seostumise kineetikat mitte-radioaktiivsete ainete juuresolekul. Tulemusena saadi reporterligandi valgule seondumise näivad kiiruskonstandid, mille väärtusi mõjutasid märgistamata ligandid. Saadud sõltuvused võimaldasid iseloomustada valguga seondumise mehhanismi.

Eksperimentaalsete tulemuste interpreteerimise lihtsustamiseks koostati kahe ligandi samaaegset seondumist kirjeldav üldskeem, mille põhjal tuletati harilike diferentsiaalvõrrandite süsteem, mida omakorda lahendati numbriliselt. Tulemusena saadi ligandi seondumist valgule kirjeldavad simulatsioonikõverad, millest koostati märgistamata ligandi kontsentratsiooni ja näilise kiiruskonstandi vahelised sõltuvused. Formuleeriti reeglid, mis võimaldavad eristada reaktsioonimehhanisme, mis erinevad ligand-valk kompleksi aeglase isomerisatsiooni esinemise poolest peale kiire sidumise staadiumit.

Mõned isomerisatsiooni initsieerivad ligandid näitasid mittehüperboolset kineetikat, mis tähendab et kõrgemate ligandi kontsentratsioonide juures tuvastati näilise kiiruskonstandi langust. See nähtus on sarnane ensüümkineetikast teada oleva substraatpidurdusega, ning viitab asjaolule, et need ligandid võivad toimida DAT-i alternatiivse sidumistsentriga. See avab uusi võimalusi selle sihtmärkvalguga toimivate ainete loomiseks.

Ainuüksi nortropaani derivaatide *N*-asendaja varieerimine muutis DAT afiinsust 3–321 nM ning selles derivaatide reas muutus ka reaktsioonimehhanism. Kiirelt ja aeglaselt seostuvate mehhanismide eristamine võimaldab kirjeldada isomerisatsiooni osa nende toime efektiivsuses. Kõik käesolevas töös analüüsitud ligandid, mille inhibeerimiskonstant oli alla 10 nM, moodustasid aeglaselt dissotsieeruva kompleksi. See viitab isomerisatsiooni olulisusele kõrge bioaktiivsusega ühendites seas. Seondudes DATiga moodustavad tõenäoliselt kõik kõrge DAT afiinsusega inhibiitorid aeglase isomerisatsiooni staadiumi, mistõttu on lisastaadiumi efekti suurendamine üks võimalustest ligandide aktiivsuste tõstmiseks. Aeglane staadium, pärast esmast kiiret seondumist, esineb ka mitmete teiste ligand-valk süsteemide korral, mistõttu oleks ka siis võimalik rakendada kineetilisi uuringuid, et tuvastada isomerisatsiooni roll.

Biomembraani integreeritud DAT-i stabiilsuse uuringud temperatuuri suhtes võimaldasid arvutada valgu inaktivatsiooni aktivatsioonienergia. Saadud aktivatsioonienergia väärtusi võrreldi teiste kirjanduses olevate membraan-ja lahustuvate valkude väärtustega ning ilmnes positiivne korrelatsioon, mis tähendab, et valgu molekulmassi suurenedes suurenes ka inaktivatsiooni aktivatsioonienergia. Kusjuures membraanvalgud olid tunduvalt vähem stabiilsemad kui sarnaste suurustega lahustuvad valgud. See kinnitab membraani olulisust DAT stabiilsusele ning ka suure tõenäosusega valgu funktsioonile.

REFERENCES

(1) Kristensen, A. S.; Andersen, J.; Jørgensen, T. N.; Sørensen, L.; Eriksen, J.; Loland, C. J.; Strømgaard, K.; Gether, U. SLC6 neurotransmitter transporters: structure, function, and regulation. *Pharmacol. Rev.* **2011**, *63*, 585–640.

(2) Langley, J. N. On the reaction of cells and of nerve-endings to certain poisons, chiefly as regards the reaction of striated muscle to nicotine and to curari. *J. Physiol.* **1905**, *33*, 374–413.

(3) Langley, J. N. On the contraction of muscle, chiefly in relation to the presence of "receptive" substances: Part III. The reaction of frog's muscle to nicotine after denervation. *J. Physiol.* **1908**, *37*, 285–300.

(4) Hill, A. V. The mode of action of nicotine and curari, determined by the form of the contraction curve and the method of temperature coefficients. *J. Physiol.* **1909**, *39*, 361–373.

(5) Middleton, R. E.; Cohen, J. B. Mapping of the Acetylcholine Binding Site of the Nicotinic Acetylcholine Receptor: [3H]Nicotine as an Agonist Photoaffinity Label? *Biochemistry* **1991**, *30*, 6987–6997.

(6) Weiland, G.; Georgia, B.; Lappi, S.; Chignell, C. F.; Taylor, P. Kinetics of agonist-mediated transitions in state of the cholinergic receptor. *J. Biol. Chem.* **1977**, *252*, 7648–7656.

(7) Neumann, E.; Chang, H. W. Dynamic properties of isolated acetylcholine receptor protein: kinetics of the binding of acetylcholine and Ca ions. *Proc. Natl. Acad. Sci. U. S. A.* **1976**, *73*, 3994–3998.

(8) Quast, U.; Schimerlik, M.; Lee, T.; Witzemann, V.; Blanchard, S.; Raftery, M. A. Ligand-induced conformation changes in Torpedo californica membrane-bound acetylcholine receptor. *Biochemistry* **1978**, *17*, 2405–2414.

(9) Strickland, S.; Palmer, G.; Massey, V. Determination of dissociation constants and specific rate constants of enzyme-substrate (or protein-ligand) interactions from rapid reaction kinetic data. *J. Biol. Chem.* **1975**, *250*, 4048–4052.

(10) Järv, J.; Hedlund, B.; Bartfai, T. Isomerization of the muscarinic receptor . antagonist complex. *J. Biol. Chem.* **1979**, *254*, 5595–5598.

(11) Dowling, M. R.; Charlton, S. J. Quantifying the association and dissociation rates of unlabelled antagonists at the muscarinic M3 receptor. *Br. J. Pharmacol.* **2006**, *148*, 927–937.

(12) Lepiku, M.; Rinken, A.; Järv, J.; Fuxe, K. Kinetic evidence for isomerization of the dopamine receptor-raclopride complex. *Neurochem. Int.* **1996**, *28*, 591–595.

(13) Stepanov, V.; Järv, J. Slow isomerization step in the interaction between mouse dopamine transporter and dopamine re-uptake inhibitor N-(3-iodoprop-2E-enyl)-2β-carbo-[3H]methoxy-3β-(4′-methylphenyl)nortropane. *Neurosci. Lett.* **2006**, *410*, 219–221.

(14) Kukk, S.; Järv, J. Differentiating between drugs with short and long residence times. *Medchemcomm* **2016**, *7*, 1654–1656.

(15) Copeland, R. A.; Pompliano, D. L.; Meek, T. D. Drug–target residence time and its implications for lead optimization. *Nat. Rev. Drug Discov.* **2006**, *5*, 730–739.

(16) Copeland, R. A. The drug-target residence time model: a 10-year retrospective. *Nat. Rev. Drug Discov.* **2016**, *15*, 87–95.

(17) Schuetz, D. A.; de Witte, W. E. A.; Wong, Y. C.; Knasmueller, B.; Richter, L.; Kokh, D. B.; Sadiq, S. K.; Bosma, R.; Nederpelt, I.; Heitman, L. H.; Segala, E.; Amaral, M.; Guo, D.; Andres, D.; Georgi, V.; Stoddart, L. A.; Hill, S.; Cooke, R.

M.; De Graaf, C.; Leurs, R.; Frech, M.; Wade, R. C.; de Lange, E. C. M.; IJzerman, A. P.; Müller-Fahrnow, A.; Ecker, G. F. Kinetics for Drug Discovery: an industry-driven effort to target drug residence time. *Drug Discov. Today* **2017**, *22*, 896–911.

(18) UniProt: the universal protein knowledgebase http://www.uniprot.org/uniprot/Q61327.

(19) Lohr, K. M.; Masoud, S. T.; Salahpour, A.; Miller, G. W. Membrane transporters as mediators of synaptic dopamine dynamics: implications for disease. *Eur. J. Neurosci.* **2017**, *45*, 20–33.

(20) Eriksen, J.; Jørgensen, T. N.; Gether, U. Regulation of dopamine transporter function by protein-protein interactions: New discoveries and methodological challenges. *J. Neurochem.* **2010**, *113*, 27–41.

(21) Schmitt, K. C.; Rothman, R. B.; Reith, M. E. A. Nonclassical Pharmacology of the Dopamine Transporter: Atypical Inhibitors, Allosteric Modulators, and Partial Substrates. *J. Pharmacol. Exp. Ther.* **2013**, *346*, 2–10.

(22) Yamashita, A.; Singh, S. K.; Kawate, T.; Jin, Y.; Gouaux, E. Crystal structure of a bacterial homologue of Na+/Cl – dependent neurotransmitter transporters. *Nature* **2005**, *437*, 215–223.

(23) Beuming, T.; Kniazeff, J.; Bergmann, M. L.; Shi, L.; Gracia, L.; Raniszewska, K.; Newman, A. H.; Javitch, J. A.; Weinstein, H.; Gether, U.; Loland, C. J. The binding sites for cocaine and dopamine in the dopamine transporter overlap. *Nat. Neurosci.* **2008**, *11*, 780–789.

(24) Indarte, M.; Madura, J. D.; Surratt, C. K. Dopamine transporter comparative molecular modeling and binding site prediction using the LeuTAa leucine transporter as a template. *Proteins Struct. Funct. Bioinforma.* **2008**, *70*, 1033–1046.

(25) Huang, X.; Gu, H. H.; Zhan, C.-G. Mechanism for Cocaine Blocking the Transport of Dopamine: Insights from Molecular Modeling and Dynamics Simulations. *J. Phys. Chem. B* **2009**, *113*, 15057–15066.

(26) Penmatsa, A.; Wang, K. H.; Gouaux, E. X-ray structure of dopamine transporter elucidates antidepressant mechanism. *Nature* **2013**, *503*, 85–90.

(27) Cheng, M. H.; Block, E.; Hu, F.; Cobanoglu, M. C.; Sorkin, A.; Bahar, I. Insights into the Modulation of Dopamine Transporter Function by Amphetamine, Orphenadrine, and Cocaine Binding. *Front. Neurol.* **2015**, *6*, 134.

(28) Wang, K. H.; Penmatsa, A.; Gouaux, E. Neurotransmitter and psychostimulant recognition by the dopamine transporter. *Nature* **2015**, *521*, 322–327.

(29) Schmitt, K. C.; Zhen, J.; Kharkar, P.; Mishra, M.; Chen, N.; Dutta, A. K.; Reith, M. E. A. Interaction of cocaine-, benztropine-, and GBR12909-like compounds with wild-type and mutant human dopamine transporters: molecular features that differentially determine antagonist-binding properties. *J. Neurochem.* **2008**, *107*, 928–940.

(30) Chen, N.; Vaughan, R. A.; Reith, M. E. A. The role of conserved tryptophan and acidic residues in the human dopamine transporter as characterized by site-directed mutagenesis. *J. Neurochem.* **2001**, *77*, 1116–1127.

(31) Riss, P. J.; Hummerich, R.; Schloss, P. Synthesis and monoamine uptake inhibition of conformationally constrained 2beta-carbomethoxy-3beta-phenyl tropanes. *Org. Biomol. Chem.* **2009**, *7*, 2688–2698.

(32) Motel, W. C.; Healy, J. R.; Viard, E.; Pouw, B.; Martin, K. E.; Matsumoto, R. R.; Coop, A. Chlorophenylpiperazine analogues as high affinity dopamine transporter ligands. *Bioorg. Med. Chem. Lett.* **2013**, *23*, 6920–6922.

(33) Prisinzano, T.; Greiner, E.; Johnson, E. M.; Dersch, C. M.; Marcus, J.; Partilla, J. S.; Rothman, R. B.; Jacobson, A. E.; Rice, K. C. Piperidine analogues of 1-[2-[bis(4-fluorophenyl)methoxy]ethyl]-4-(3-phenylpropyl)piperazine (GBR 12909): High affinity ligands for the dopamine transporter. *J. Med. Chem.* **2002**, *45*, 4371–4374.

(34) Dutta, A. K.; Davis, M. C.; Fei, X.-S.; Beardsley, P. M.; Cook, C. D.; Reith, M. E. A. Expansion of structure− activity studies of piperidine analogues of 1-[2-(diphenylmethoxy) ethyl]-4-(3-phenylpropyl) piperazine (GBR 12935) compounds by altering substitutions in the N-benzyl moiety and behavioral pharmacology of selected molecules. *J. Med. Chem.* **2002**, *45*, 654–662.

(35) Zhang, Y.; Rothman, R. B.; Dersch, C. M.; De Costa, B. R.; Jacobson, A. E.; Rice, K. C. Synthesis and transporter binding properties of bridged piperazine analogues of 1-{2-[bis(4-fluorophenyl)methoxy]ethyl}-4-(3-phenylpropyl)piperazine (GBR 12909). *J. Med. Chem.* **2000**, *43*, 4840–4849.

(36) Matecka, D.; Rothman, R. B.; Radesca, L.; de Costa, B. R.; Dersch, C. M.; Partilla, J. S.; Pert, A.; Glowa, J. R.; Wojnicki, F. H.; Rice, K. C. Development of novel, potent, and selective dopamine reuptake inhibitors through alteration of the piperazine ring of 1-[2-(diphenylmethoxy)ethyl]-and 1-[2-[bis(4-fluorophenyl)methoxy]ethyl]-4-(3-phenylpropyl)piperazines (GBR 12935 and GBR 12909). *J. Med. Chem.* **1996**, *39*, 4704–4716.

(37) Matecka, D.; Lewis, D.; Rothman, R. B.; Dersch, C. M.; Wojnicki, F. H. E.; Glowa, J. R.; DeVries, A. C.; Pert, A.; Rice, K. C. Heteroaromatic analogs of 1-[2-(diphenylmethoxy)ethyl]- and 1-[2- [bis(4-fluorophenyl)methoxy]ethyl]-4-(3-phenylpropyl)piperazines (GBR 12935 and GBR 12909) as high-affinity dopamine reuptake inhibitors. *J. Med. Chem.* **1997**, *40*, 705–716.

(38) Preti, A. REVIEW: New developments in the pharmacotherapy of cocaine abuse. *Addict. Biol.* **2007**, *12*, 133–151.

(39) Cao, J.; Slack, R. D.; Bakare, O. M.; Burzynski, C.; Rais, R.; Slusher, B. S.; Kopajtic, T.; Bonifazi, A.; Ellenberger, M. P.; Yano, H.; He, Y.; Bi, G.-H.; Xi, Z.-X.; Loland, C. J.; Newman, A. H. Novel and High Affinity 2-[(Diphenylmethyl)sulfinyl]acetamide (Modafinil) Analogues as Atypical Dopamine Transporter Inhibitors. *J. Med. Chem.* **2016**, *59*, 10676–10691.

(40) Maurice, T.; Su, T. P. The pharmacology of sigma-1 receptors. *Pharmacol. Ther.* **2009**, *124*, 195–206.

(41) Katz, J. L.; Libby, T. A.; Kopajtic, T.; Husbands, S. M.; Newman, A. H. Behavioral effects of rimcazole analogues alone and in combination with cocaine. *Eur. J. Pharmacol.* **2003**, *468*, 109–119.

(42) Gelenberg, A. J.; Van Putten, T.; Lavori, P. W.; Wojcik, J. D.; Falk, W. E.; Marder, S.; Galvin-Nadeau, M.; Spring, B.; Mohs, R. C.; Brotman, A. W. Anticholinergic effects on memory: benztropine versus amantadine. *J. Clin. Psychopharmacol.* **1989**, *9*, 180–185.

(43) Hiranita, T.; Hong, W. C.; Kopajtic, T.; Katz, J. L. Sigma Receptor Effects of N-Substituted Benztropine Analogs: Implications for Antagonism of Cocaine Self Administration. *J. Pharmacol. Exp. Ther.* **2017**, *362*, 2–13.

(44) Kulkarni, S. S.; Grundt, P.; Kopajtic, T.; Katz, J. L.; Newman, A. H. Structure − Activity Relationships at Monoamine Transporters for a Series of N-Substituted 3α-(Bis[4-fluorophenyl]methoxy)tropanes: Comparative Molecular Field Analysis, Synthesis, and Pharmacological Evaluation. *J. Med. Chem.* **2004**, *47*, 3388–3398.

(45) Banister, S. D.; Moussa, I. A.; Beinat, C.; Reynolds, A. J.; Schiavini, P.; Jorgensen, W. T.; Kassiou, M. Trishomocubane as a scaffold for the development of selective dopamine transporter (DAT) ligands. *Bioorg. Med. Chem. Lett.* **2011**, *21*, 38–41.
(46) Enyedy, I. J.; Sakamuri, S.; Zaman, W. A.; Johnson, K. M.; Wang, S. Pharmacophore-based discovery of substituted pyridines as novel dopamine transporter inhibitors. *Bioorganic Med. Chem. Lett.* **2003**, *13*, 513–517.
(47) Schmitt, K. C.; Mamidyala, S.; Biswas, S.; Dutta, A. K.; Reith, M. E. A. Bivalent phenethylamines as novel dopamine transporter inhibitors: evidence for multiple substrate-binding sites in a single transporter. *J. Neurochem.* **2010**, *112*, 1605–1618.
(48) Wang, S.; Sakamuri, S. (4-methylphenyl)-3-piperidyl 4-methylphenyl ketone, as a potential cocaine antagonist through 3D-database pharmacophore searching. Molecular modeling, structure. *J. Med. Chem.* **2000**, *43*, 351–360.
(49) He, X. S.; Raymon, L. P.; Mattson, M. V.; Eldefrawi, M. E.; de Costa, B. R. Synthesis and biological evaluation of 1-[1-(2-benzo[b]thienyl)cyclohexyl]-piperidine homologs at dopamine-uptake and phencyclidine-, and .sigma.-binding sites. *J. Med. Chem.* **1993**, *36*, 1188–1193.
(50) Meltzer, P. C.; Wang, P.; Blundell, P.; Madras, B. K. Synthesis and evaluation of dopamine and serotonin transporter inhibition by oxacyclic and carbacyclic analogues of methylphenidate. *J. Med. Chem.* **2003**, *46*, 1538–1545.
(51) He, X.; Raymon, L. P.; Mattson, M. V.; Eldefrawi, M. E.; de Costa, B. R. Further studies of the structure-activity relationships of 1-[1-(2-benzo[b]thienyl)-cyclohexyl]piperidine. Synthesis and evaluation of 1-(2-benzo[b]thienyl)-N,N-dialkylcyclohexylamines at dopamine uptake and phencyclidine binding sites. *J. Med. Chem.* **1993**, *36*, 4075–4081.
(52) Runyon, S. P.; Carroll, F. I. Tropane-based dopamine transporter-uptake inhibitors. In *Dopamine Transporters, Chemistry, Biology, and Pharmacology. Wiley, New York*; 2008; pp. 125–170.
(53) Carroll, F.; Lewin, A.; Boja, J. W.; Kuhar, M. J. Cocaine receptor: biochemical characterization and structure-activity relationships of cocaine analogs at the dopamine transporter. *J. Med. Chem.* **1992**, *35*, 969–981.
(54) Clarke, R.; Daum, S.; Gambino, A.; Aceto, M.; Pearl, J.; Levitt, M.; Cuminskey, W.; Bogado, E. Compounds Affecting the Central Nervous System. 4. 3.β-Phenyltropane-2-carboxylic Esters and Analogs. *J. Med. Chem.* **1973**, *16*, 1260–1267.
(55) Carroll, F. I.; Gao, Y. G.; Rahman, M. A.; Abraham, P.; Parham, K.; Lewin, A. H.; Boja, J. W.; Kuhar, M. J. Synthesis, ligand binding, QSAR, and CoMFA study of 3β-(p-substituted phenyl)tropane-2 β-carboxylic acid methyl esters. *J. Med. Chem.* **1991**, *34*, 2719–2725.
(56) Ritz, M. C.; Lamb, R. J.; Goldberg, S. R.; Kuhar, M. J. Cocaine receptors on dopamine transporters are related to self-administration of cocaine. *Science* **1987**, *237*, 1219–1223.
(57) Carroll, F. I.; Gao, Y.; Abraham, P.; Lewin, a H.; Lew, R.; Patel, A.; Boja, J. W.; Kuhar, M. J. Probes for the cocaine receptor. Potentially irreversible ligands for the dopamine transporter. *J. Med. Chem.* **1992**, *35*, 1813–1817.
(58) Zou, M. F.; Kopajtic, T.; Katz, J. L.; Wirtz, S.; Justice, J. B.; Newman, a H. Novel tropane-based irreversible ligands for the dopamine transporter. *J. Med. Chem.* **2001**, *44*, 4453–4461.

(59) Wang, L. C.; Berfield, J. L.; Kuhar, M. J.; Carroll, F. I.; Reith, M. E. A. RTI-76, an isothiocynate derivative of a phenyltropane cocaine analog, as a tool for irreversibly inactivating dopamine transporter function in vitro. *Naunyn. Schmiedebergs. Arch. Pharmacol.* **2000**, *362*, 238–247.
(60) Carroll, F. I. 2002 Medicinal Chemistry Division Award address: monoamine transporters and opioid receptors. Targets for addiction therapy. *J. Med. Chem.* **2003**, *46*, 1775–1794.
(61) Carroll, F. I.; Gray, J. L.; Abraham, P.; Kuzemko, M. A.; Lewin, A. H.; Boja, J. W.; Kuhar, M. J. 3-Aryl-2-(3'-substituted-1',2',4'-oxadiazol-5'-yl)tropane analogues of cocaine: Affinities at the cocaine binding site at the dopamine, serotonin, and norepinephrine transporters. *J. Med. Chem.* **1993**, *36*, 2886–2890.
(62) Keverline-Frantz, K. I.; Boja, J. W.; Kuhar, M. J.; Abraham, P.; Burgess, J. P.; Lewin, a H.; Carroll, F. I. Synthesis and ligand binding of tropane ring analogues of paroxetine. *J. Med. Chem.* **1998**, *41*, 247–257.
(63) Peng, X.; Zhang, A.; Kula, N. S.; Baldessarini, R. J.; Neumeyer, J. L. Synthesis and amine transporter affinities of novel phenyltropane derivatives as potential positron emission tomography (PET) imaging agents. *Bioorg. Med. Chem. Lett.* **2004**, *14*, 5635–5639.
(64) Jin, C.; Navarro, H. a; Carroll, F. I. Synthesis and receptor binding properties of 2β-alkynyl and 2β-(1,2,3-triazol)substituted 3β-(substituted phenyl)tropane derivatives. *Bioorg. Med. Chem.* **2008**, *16*, 5529–5535.
(65) Hong, W. C.; Kopajtic, T. A.; Xu, L.; Lomenzo, S. A.; Jean, B.; Madura, J. D.; Surratt, C. K.; Trudell, M. L.; Katz, J. L. 2-Substituted 3 –Aryltropane Cocaine Analogs Produce Atypical DAT Inhibitor Effects Without Inducing Inward-Facing DAT Conformations. *J. Pharmacol. Exp. Ther.* **2016**, *46208*, 624–634.
(66) Kotian, P.; Mascarella, S. W.; Abraham, P.; Lewin, a H.; Boja, J. W.; Kuhar, M. J.; Carroll, F. I. Synthesis, ligand binding, and quantitative structure-activity relationship study of 3β-(4'-substituted phenyl)-2β-heterocyclic tropanes: evidence for an electrostatic interaction at the 2β-position. *J. Med. Chem.* **1996**, *39*, 2753–2763.
(67) Nielsen, S.; Pedersen, C. M.; Hansen, S. G.; Petersen, M. D.; Sinning, S.; Wiborg, O.; Jensen, H. H.; Bols, M. An extended study of dimeric phenyl tropanes. *Bioorg. Med. Chem.* **2009**, *17*, 4900–4909.
(68) Blough, B. E.; Keverline, K. I.; Nie, Z.; Navarro, H.; Kuhar, M. J.; Carroll, F. I. Synthesis and Transporter Binding Properties of 3β-[4'-(Phenylalkyl, -phenylalkenyl, and -phenylalkynl)phenyl]tropane-2β-carboxylic Acid Methyl Esters: Evidence of a Remote Phenyl Binding Domain on the Dopamine Transporter. *J. Med. Chem.* **2002**, *45*, 4029–4037.
(69) Blough, B. E.; Abraham, P.; Lewin, a H.; Kuhar, M. J.; Boja, J. W.; Carroll, F. I. Synthesis and transporter binding properties of 3β-(4'-alkyl-, 4'-alkenyl-, and 4' -alkynylphenyl)nortropane-2β-carboxylic acid methyl esters: serotonin transporter selective analogs. *J. Med. Chem.* **1996**, *39*, 4027–4035.
(70) Blough, B. E.; Abraham, P.; Mills, A. C.; Lewin, A. H.; Boja, J. W.; Scheffel, U.; Kuhar, M. J.; Carroll, F. I. 3β-(4-ethyl-3-iodophenyl)nortropane-2β-carboxylic acid methyl ester as a high-affinity selective ligand for the serotonin transporter. *J. Med. Chem.* **1997**, *40*, 3861–3864.
(71) Stoelwinder, J.; Roberti, M.; Kozikowski, A. P.; Johnson, K. M.; Bergmann, J. S. Differential binding and dopamine uptake activity of cocaine analogues modified at nitrogen. *Bioorg. Med. Chem. Lett.* **1994**, *4*, 303–308.

(72) Neumeyer, J. L.; Tamagnan, G.; Wang, S.; Gao, Y.; Milius, R. A.; Kula, N. S.; Baldessarini, R. J. N-Substituted Analogs of 2β-Carbomethoxy-3β-(4‘-iodophenyl)tropane (β-CIT) with Selective Affinity to Dopamine or Serotonin Transporters in Rat Forebrain. *J. Med. Chem.* **1996**, *39*, 543–548.

(73) Emond, P.; Garreau, L.; Chalon, S.; Boazi, M.; Caillet, M.; Bricard, J.; Frangin, Y.; Mauclaire, L.; Besnard, J.; Guilloteau, D. Synthesis and Ligand Binding of Nortropane Derivatives: N-Substituted 2β-Carbomethoxy-3β-(4‘-iodophenyl)-nortropane and N-(3-Iodoprop-(2E)-enyl)-2β-carbomethoxy-3β-(3‘,4‘-disubstituted phenyl)nortropane. New High-Affinity and Selective Compounds for the Do. *J. Med. Chem.* **1997**, *2623*, 1366–1372.

(74) Abraham, P.; Pitner, J. B.; Lewin, a H.; Boja, J. W.; Kuhar, M. J.; Carroll, F. I. N-modified analogues of cocaine: synthesis and inhibition of binding to the cocaine receptor. *J. Med. Chem.* **1992**, *35*, 141–144.

(75) Aronson, B.; Enmon, J. L.; Izenwasser, S.; Katz, J. L.; Kelkar, S. V; Luo, L.; Nolan, S. P.; Trudell, M. L. Synthesis and ligand binding of eta(6)-(2beta-carbomethoxy-3beta-phenyltropane) transition metal complexes. *J. Med. Chem.* **1996**, *39*, 1560–1563.

(76) Meltzer, P. C.; Liang, A. Y.; Blundell, P.; Gonzalez, M. D.; Chen, Z.; George, C.; Madras, B. K. 2-Carbomethoxy-3-aryl-8-oxabicyclo [3.2. 1] octanes: potent non-nitrogen inhibitors of monoamine transporters. *J. Med. Chem.* **1997**, *40*, 2661–2673.

(77) Meltzer, P. C.; Blundell, P.; Yong, Y. F.; Chen, Z.; George, C.; Gonzalez, M. D.; Madras, B. K. 2-carbomethoxy-3-aryl-8-bicyclo[3.2.1]octanes: Potent non-nitrogen inhibitors of monoamine transporters. *J. Med. Chem.* **2000**, *43*, 2982–2991.

(78) Calligaro, D. O.; Eldefrawi, M. E. High Affinity Stereospecific Binding of [3H] Cocaine in Striatum and its Relationship to the Dopamine Transporter. *Membr. Biochem.* **1987**, *7*, 87–106.

(79) Madras, B. K.; Spealman, R. D.; Fahey, M. A.; Neumeyer, J. L.; Saha, J. K.; Milius, R. A. Cocaine receptors labeled by [3H] 2β-carbomethoxy-3β-(4-fluorophenyl) tropane. *Mol. Pharmacol.* **1989**, *36*, 518–524.

(80) Scheffel, U.; Pögün, S.; Stathis, M.; Boja, J. W.; Kuhar, M. J. In vivo labeling of cocaine binding sites on dopamine transporters with [3H]WIN 35,428. *J. Pharmacol. Exp. Ther.* **1991**, *257*, 954–958.

(81) Ritz, M. C.; Boja, J. W.; Grigoriadis, D.; Zaczek, R.; Carroll, F. I.; Lewis, A. H.; Kuhar, M. J. [3H]WIN 35,065–2: A Ligand for Cocaine Receptors in Striatum. *J. Neurochem.* **1990**, *55*, 1556–1562.

(82) Boja, J. W.; Mitchell, W. M.; Patel, A.; Kopajtic, T. A.; Carroll, F. I.; Lewin, A. H.; Abraham, P.; Kuhar, M. J. High-affinity binding of [125I]RTI-55 to dopamine and serotonin transporters in rat brain. *Synapse* **1992**, *12*, 27–36.

(83) Chalon, S.; Garreau, L.; Emond, P.; Zimmer, L.; Vilar, M. P.; Besnard, J. C.; Guilloteau, D. Pharmacological characterization of (E)-N-(3-iodoprop-2-enyl)-2β-carbomethoxy-3β-(4′-methylphenyl) nortropane as a selective and potent inhibitor of the neuronal. *J. Pharmacol. Exp. Ther.* **1999**, *291*, 648–654.

(84) Lomenzo, S. A.; Izenwasser, S.; Katz, J. L.; Terry, P. D.; Zhu, N.; Klein, C. L.; Trudell, M. L. Synthesis, structure, dopamine transporter affinity, and dopamine uptake inhibition of 6-alkyl-3-benzyl-2-[(methoxycarbonyl)methyl]tropane derivatives. *J. Med. Chem.* **1997**, *40*, 4406–4414.

(85) Halldin, C.; Erixon-Lindroth, N.; Pauli, S.; Chou, Y.-H.; Okubo, Y.; Karlsson, P.; Lundkvist, C.; Olsson, H.; Guilloteau, D.; Emond, P.; Farde, L. [11 C]PE2I: a

highly selective radioligand for PET examination of the dopamine transporter in monkey and human brain. *Eur. J. Nucl. Med. Mol. Imaging* **2003**, *30*, 1220–1230.

(86) Stepanov, V.; Krasikova, R.; Raus, L.; Loog, O.; Hiltunen, J.; Halldin, C. An efficient one-step radiosynthesis of [18F]FE-PE2I, a PET radioligand for imaging of dopamine transporters. *J. Label. Compd. Radiopharm.* **2012**, *55*, 206–210.

(87) Dollé, F.; Emond, P.; Mavel, S.; Demphel, S.; Hinnen, F.; Mincheva, Z.; Saba, W.; Valette, H.; Chalon, S.; Halldin, C.; Helfenbein, J.; Legaillard, J.; Madelmont, J.-C.; Deloye, J.-B.; Bottlaender, M.; Guilloteau, D. Synthesis, radiosynthesis and in vivo preliminary evaluation of [11C]LBT-999, a selective radioligand for the visualisation of the dopamine transporter with PET. *Bioorg. Med. Chem.* **2006**, *14*, 1115–1125.

(88) Tossici-Bolt, L.; Dickson, J. C.; Sera, T.; Booij, J.; Asenbaun-Nan, S.; Bagnara, M. C.; Borght, T. Vander; Jonsson, C.; de Nijs, R.; Hesse, S.; Koulibaly, P. M.; Akdemir, U. O.; Koole, M.; Tatsch, K.; Varrone, A. [123I]FP-CIT ENC-DAT normal database: the impact of the reconstruction and quantification methods. *EJNMMI Phys.* **2017**, *4*, 8.

(89) Brooks, D. J. Molecular imaging of dopamine transporters. *Ageing Res. Rev.* **2016**, *30*, 114–121.

(90) Rasmussen, S. G. F.; Carroll, F. I.; Maresch, M. J.; Jensen, A. D.; Tate, C.G.; Gether, U. Biophysical characterization of the cocaine binding pocket in the serotonin transporter using a fluorescent cocaine analogue as a molecular reporter. *J. Biol. Chem.* **2001**, *276*, 4717–4723.

(91) Cha, J. H.; Zou, M. F.; Adkins, E. M.; Rasmussen, S. G. F.; Loland, C. J.; Schoenenberger, B.; Gether, U.; Newman, A. H. Rhodamine-labeled 2β-carbomethoxy-3β-(3,4-dichlorophenyl)tropane analogues as high-affinity fluorescent probes for the dopamine transporter. *J. Med. Chem.* **2005**, *48*, 7513–7516.

(92) Rasmussen, S. G. F.; Adkins, E. M.; Carroll, F. I.; Maresch, M. J.; Gether, U. Structural and functional probing of the biogenic amine transporters by fluorescence spectroscopy. *Eur. J. Pharmacol.* **2003**, *479*, 13–22.

(93) Anderluh, A.; Klotzsch, E.; Reismann, A. W. A. F.; Brameshuber, M.; Kudlacek, O.; Newman, A. H.; Sitte, H. H.; Schütz, G. J. Single molecule analysis reveals coexistence of stable serotonin transporter monomers and oligomers in the live cell plasma membrane. *J. Biol. Chem.* **2014**, *289*, 4387–94.

(94) Vuorenpää, A.; Jørgensen, T. N.; Newman, A. H.; Madsen, K. L.; Scheinin, M.; Gether, U. Differential internalization rates and postendocytic sorting of the norepinephrine and dopamine transporters are controlled by structural elements in the N termini. *J. Biol. Chem.* **2016**, *291*, 5634–5651.

(95) Ketelslegers, J. M.; Knott, G. D.; Catt, K. J. Kinetics of gonadotropin binding by receptors by the rat testis. Analysis by a nonlinear curve-fitting method. *Biochemistry* **1975**, *14*, 3075–3083.

(96) Motulsky, H. J.; Mahan, L. C. The kinetics of competitive radioligand binding predicted by the law of mass action. *Mol. Pharmacol.* **1984**, *25*, 1–9.

(97) Wanant, S.; Quon, M. J. Insulin Receptor Binding Kinetics: Modeling and Simulation Studies. *J. Theor. Biol.* **2000**, *205*, 355–364.

(98) Wittmann, H.-J.; Strasser, A. Competitive association binding kinetic assays: a new tool to detect two different binding orientations of a ligand to its target protein under distinct conditions? *Naunyn. Schmiedebergs. Arch. Pharmacol.* **2017**, 1–18.

(99) Bruning, J. B.; Parent, A. A.; Gil, G.; Zhao, M.; Nowak, J.; Pace, M. C.; Smith, C. L.; Afonine, P. V; Adams, P. D.; Katzenellenbogen, J. A.; Nettles, K. W. Coupling of receptor conformation and ligand orientation determine graded activity. *Nat. Chem. Biol.* **2010**, *6*, 837–843.
(100) Bock, A.; Chirinda, B.; Krebs, F.; Messerer, R.; Bätz, J.; Muth, M.; Dallanoce, C.; Klingenthal, D.; Tränkle, C.; Hoffmann, C. Dynamic ligand binding dictates partial agonism at a G protein–coupled receptor. *Nat. Chem. Biol.* **2014**, *10*, 18–20.
(101) Kirifides, A.; Harvey, J.; Aloyo, V. The low affinity binding site for the cocaine analog, WIN 35, 428 is an artifact of freezing caudate tissue. *Life Sci.* **1992**, *50*, 139–142.
(102) Hasenhuetl, P. S.; Schicker, K.; Koenig, X.; Li, Y.; Sarker, S.; Stockner, T.; Sucic, S.; Sitte, H. H.; Freissmuth, M.; Sandtner, W. Ligand Selectivity among the Dopamine and Serotonin Transporters Specified by the Forward Binding Reaction. *Mol. Pharmacol.* **2015**, *88*, 12–18.
(103) Stepanov, V. Slow conformational changes in dopamine transporter interaction with its ligands, University of Tartu, 2009.
(104) Stepanov, V.; Järv, J. Kinetic mechanism of dopamine transporter interaction with 1-(2-(bis-(4-fluorophenyl)methoxy)ethyl)-4-(3-phenylpropyl)piperazine (GBR 12909). *Neurochem. Int.* **2008**, *53*, 370–373.
(105) Appel, L.; Jonasson, M.; Danfors, T.; Nyholm, D.; Askmark, H.; Lubberink, M.; Sörensen, J. Use of 11C-PE2I PET in Differential Diagnosis of Parkinsonian Disorders. *J. Nucl. Med.* **2015**, *56*, 234–242.
(106) Rajarathnam, K.; Rösgen, J. Isothermal titration calorimetry of membrane proteins – Progress and challenges. *Biochim. Biophys. Acta – Biomembr.* **2014**, *1838*, 69–77.
(107) Siligardi, G.; Hussain, R.; Patching, S. G.; Phillips-Jones, M. K. Ligand- and drug-binding studies of membrane proteins revealed through circular dichroism spectroscopy. *Biochim. Biophys. Acta – Biomembr.* **2014**, *1838*, 34–42.
(108) Whited, A. M.; Park, P. S.-H. Atomic force microscopy: A multifaceted tool to study membrane proteins and their interactions with ligands. *Biochim. Biophys. Acta – Biomembr.* **2014**, *1838*, 56–68.
(109) Poget, S. F.; Girvin, M. E. Solution NMR of membrane proteins in bilayer mimics: Small is beautiful, but sometimes bigger is better. *Biochim. Biophys. Acta – Biomembr.* **2007**, *1768*, 3098–3106.
(110) Wilzbach, K. E. Tritium-Labeling By Exposure of Organic Compounds To Tritium Gas. *J. Am. Chem. Soc.* **1957**, *79*, 1013–1013.
(111) Paton, W. D.; Rang, H. P. The uptake of atropine and related drugs by intestinal smooth muscle of the guinea-pig in relation to acetylcholine receptors. *Proc. R. Soc. London. Ser. B, Biol. Sci.* **1965**, *163*, 1–44.
(112) Christopoulos, A.; Lanzafame, A.; Ziegler, A.; Mitchelson, F. Kinetic studies of co-operativity at atrial muscarinic M2 receptors with an “infinite dilution” procedure. *Biochem. Pharmacol.* **1997**, *53*, 795–800.
(113) Kloog, Y.; Sokolovsky, M. Muscarinic binding to mouse brain receptor sites. *Biochem. Biophys. Res. Commun.* **1978**, *81*, 710–717.
(114) Vauquelin, G.; Szczuka, A. Kinetic versus allosteric mechanisms to explain insurmountable antagonism and delayed ligand dissociation. *Neurochem. Int.* **2007**, *51*, 254–260.
(115) Stepanov, V.; Schou, M.; Järv, J.; Halldin, C. Synthesis of 3H-labeled N-(3-iodoprop-2E-enyl)-2β-carbomethoxy-3β-(4-methylphenyl)nortropane (PE2I) and

its interaction with mice striatal membrane fragments. *Appl. Radiat. Isot.* **2007**, *65*, 293–300.
(116) Järv, J.; Hedlund, B.; Bartfai, T. Kinetic studies on muscarinic antagonist-agonist competition. *J. Biol. Chem.* **1980**, *255*, 2649–2651.
(117) Cassel, J. A.; Daubert, J. D.; DeHaven, R. N. [3H]Alvimopan binding to the μ opioid receptor: Comparative binding kinetics of opioid antagonists. *Eur. J. Pharmacol.* **2005**, *520*, 29–36.
(118) Patching, S. G. Surface plasmon resonance spectroscopy for characterisation of membrane protein–ligand interactions and its potential for drug discovery. *Biochim. Biophys. Acta – Biomembr.* **2014**, *1838*, 43–55.
(119) Pattnaik, P. Surface plasmon resonance. *Appl. Biochem. Biotechnol.* **2005**, *126*, 79–92.
(120) Zhu, J.; Mactutus, C. F.; Wallace, D. R.; Booze, R. M. HIV-1 Tat protein-induced rapid and reversible decrease in [3H]dopamine uptake: dissociation of [3H]dopamine uptake and [3H]2β-carbomethoxy-3-β-(4-fluorophenyl)tropane (WIN 35,428) binding in rat striatal synaptosomes. *J Pharmacol Exp Ther* **2009**, *329*, 1071–1083.
(121) Kumbhat, S.; Shankaran, D. R.; Kim, S. J.; Gobi, K. V.; Joshi, V.; Miura, N. Surface plasmon resonance biosensor for dopamine using D3 dopamine receptor as a biorecognition molecule. *Biosens. Bioelectron.* **2007**, *23*, 421–427.
(122) Liang, W.; Wang, S.; Festa, F.; Wiktor, P.; Wang, W.; Magee, M.; Labaer, J.; Tao, N. Measurement of small molecule binding kinetics on a protein microarray by plasmonic-based electrochemical impedance imaging. *Anal. Chem.* **2014**, *86*, 9860–9865.
(123) Campbell, C. T.; Kim, G. SPR microscopy and its applications to high-throughput analyses of biomolecular binding events and their kinetics. *Biomaterials* **2007**, *28*, 2380–2392.
(124) Sridharan, R.; Zuber, J.; Connelly, S. M.; Mathew, E.; Dumont, M. E. Fluorescent approaches for understanding interactions of ligands with G protein coupled receptors. *Biochim. Biophys. Acta – Biomembr.* **2014**, *1838*, 15–33.
(125) Veiksina, S.; Kopanchuk, S.; Rinken, A. Budded baculoviruses as a tool for a homogeneous fluorescence anisotropy-based assay of ligand binding to G protein-coupled receptors: The case of melanocortin 4 receptors. *Biochim. Biophys. Acta – Biomembr.* **2014**, *1838*, 372–381.
(126) Yung-Chi, C.; Prusoff, W. H. Relationship between the inhibition constant (KI) and the concentration of inhibitor which causes 50 per cent inhibition (I50) of an enzymatic reaction. *Biochem. Pharmacol.* **1973**, *22*, 3099–3108.
(127) Chen, Z.; Izenwasser, S.; Katz, J. L.; Zhu, N.; Klein, C. L.; Trudell, M. L. Synthesis and dopamine transporter affinity of 2-(methoxycarbonyl)-9-methyl-3-phenyl-9-azabicyclo[3.3.1]nonane derivatives. *J. Med. Chem.* **1996**, *39*, 4744–4749.
(128) Davies, H.; Gilliatt, V.; Kuhn, L. Synthesis of 2β-acyl-3β-(substituted naphthyl)-8-azabicyclo octanes and their binding affinities at dopamine and serotonin transport sites. *J. Med. Chem.* **2001**, 1509–1515.
(129) Airaksinen, A. J.; Huotari, M.; Shvetsov, A.; Vainiotalo, P.; Männisto, P. T.; Tuomisto, L.; Bergström, K. a; Vepsäläinen, J. Synthesis and biological evaluation of 6/7-exo-methyl-3β-(4-iodo)phenyltropane-2β-carboxylic acid methyl esters. *Eur. J. Med. Chem.* **2005**, *40*, 299–304.

(130) Xu, L.; Trudell, M. L. Stereoselective synthesis of 2β-carbomethoxy-3β-phenyl-tropane derivatives. Enhanced stereoselectivity observed for the conjugate addition reaction of phenylmagnesium bromide derivatives with anhydro dichloromethane. *J. Heterocycl. Chem.* **1996**, *33*, 2037–2039.
(131) Moore, J. L.; Taylor, S. M.; Soloshonok, V. A. An efficient and operationally convenient general synthesis of tertiary amines by direct alkylation of secondary amines with alkyl halides in the presence of Huenig's base. *Arkivoc* **2005**, *6*, 287–292.
(132) Varfolomeev, S. D.; Zaitsev, S. V Kinetic Methods in Biochemistry. *Moscow State Univ. Moscow* **1982**.
(133) Eller, M.; Järv, J.; Palumaa, P. Influence of non-radioactive ligands on kinetics of N-methyl-[3H] scopolamine binding to muscarinic receptor. *Org React* **1988**, *25*, 372–386.
(134) Kukk, S.; Miidla, P.; Järv, J. Kinetic tools for the identification of ligand–receptor interaction mechanisms. *Proc. Est. Acad. Sci.* **2017**, *66*, 202–213.
(135) Le Bihan, T.; Gicquaud, C. Kinetic study of the thermal denaturation of G actin using differential scanning calorimetry and intrinsic fluorescence spectroscopy. *Biochem. Biophys. Res. Commun.* **1993**, *194*, 1065–1073.
(136) Arroyo-Reyna, A.; Hernández-Arana, A. The thermal denaturation of stem bromelain is consistent with an irreversible two-state model. *Biochim. Biophys. Acta (BBA)/Protein Struct. Mol.* **1995**, *1248*, 123–128.
(137) Sanchez-Ruiz, J. M.; Lopez-Lacomba, J. L.; Mateo, P. L.; Vilanova, M.; Serra, M. A.; Aviles, F. X. Analysis of the thermal unfolding of porcine procarboxy-peptidase A and its functional pieces by differential scanning calorimetry. *Eur. J. Biochem.* **1988**, *176*, 225–230.
(138) Sánchez-Ruiz, J. M.; López-Lacomba, J. L.; Cortijo, M.; Mateo, P. L. Differential scanning calorimetry of the irreversible thermal denaturation of thermolysin. *Biochemistry* **1988**, *27*, 1648–1652.
(139) Zhadan, G. G.; Shnyrov, V. L. Differential-scanning-calorimetric study of the irreversible thermal denaturation of 8 kDa cytotoxin from the sea anemone Radianthus macrodactylus. *Biochem. J.* **1994**, *299 (Pt 3*, 731–733.
(140) Potekhin, S. A.; Loseva, O. I.; Tiktopulo, E. I.; Dobritsa, A. P. Transition state of the rate-limiting step of heat denaturation of Cry3A delta-endotoxin. *Biochemistry* **1999**, *38*, 4121–4127.
(141) Shnyrov, V. L.; Martínez, L. D.; Roig, M. G.; Lyubarev, A. E.; Kurganov, B. I.; Villar, E. Irreversible thermal denaturation of lipase B from Candida rugosa. *Thermochim. Acta* **1999**, *325*, 143–149.
(142) Shin, I.; Silman, I.; Bon, C.; Weiner, L. Liposome-catalyzed unfolding of acetylcholinesterase from Bungarus fasciatus. *Biochemistry* **1998**, *37*, 4310–4316.
(143) Mall, R.; Naik, G.; Mina, U.; Mishra, S. K. Purification and characterization of a thermostable soluble peroxidase from Citrus medica leaf. *Prep. Biochem. Biotechnol.* **2013**, *43*, 137–151.
(144) Maurya, S. R.; Mahalakshmi, R. Influence of Protein – Micelle Ratios and Cysteine Residues on the Kinetic Stability and Unfolding Rates of Human Mitochondrial VDAC-2. *PLoS One* **2014**, *9*, 1–13.
(145) Langel, U.; Rinken, A.; Tähepõld, L.; Järv, J. Kinetics of the muscarinic receptor inactivation. *Neirokhimia* **1982**, 341–351.

(146) Allikalt, A.; Rinken, A. Budded baculovirus particles as a source of membrane proteins for radioligand binding assay: The case of dopamine D1 receptor. *J. Pharmacol. Toxicol. Methods* **2017**, *86*, 81–86.
(147) Ding, Y.; Liu, R.; Rong, J.; Xiong, S. Heat-induced denaturation and aggregation of actomyosin and myosin from yellowcheek carp during setting. *Food Chem.* **2014**, *149*, 237–243.
(148) Levi, V.; Rossi, J. P. F. C.; Echarte, M. M.; Castello, P. R.; González Flecha, F. L. Thermal stability of the plasma membrane calcium pump. Quantitative analysis of its dependence on lipid-protein interactions. *J. Membr. Biol.* **2000**, *173*, 215–225.
(149) Carroll, F. I.; Tyagi, S.; Blough, B. E.; Kuhar, M. J.; Navarro, H. a Synthesis and monoamine transporter binding properties of 3alpha-(substituted phenyl)-nortropane-2beta-carboxylic acid methyl esters. Norepinephrine transporter selective compounds. *J. Med. Chem.* **2005**, *48*, 3852–3857.
(150) Emond, P.; Helfenbein, J.; Chalon, S.; Garreau, L.; Vercouillie, J.; Frangin, Y.; Besnard, J. C.; Guilloteau, D. Synthesis of tropane and nortropane analogues with phenyl substitutions as serotonin transporter ligands. *Bioorg. Med. Chem.* **2001**, *9*, 1849–55.
(151) Copeland, R. A. A practical introduction to structure, mechanism, and data analysis. *Enzym. 2nd ed. John Wiley Sons, New York, NY* **2000**, 104.

ACKNOWLEDGEMENTS

I wish to express my greatest gratitude to my supervisor, prof. Jaak Järv, for his supervision, support and advice throughout these years.

I also wish to thank all the staff in PharmaSynth, especially Dr. Olavi Loog and Dr. Jukka-Veli Hiltunen, for the opportunity to participate and work on the company's projects.

Special thanks to Dr. Vladimir Stepanov for laying the groundwork of this topic, Dr. Peep Miidla for the aid in mathematical modelling and code writing and prof. Ago Rinken for the possibility to use some of Department of Biochemistry lab equipment.

I would like to acknowledge all the staff and colleagues of the Department of Organic Chemistry for their opinions and remarks.

I am very grateful to my family and those closest to me for being beside me.

PUBLICATIONS

CURRICULUM VITAE

Name:	Siim Kukk
Date of birth:	July 12, 1989
Address:	Institute of Chemistry, Ravila 14a, 50411, Tartu, Estonia
Nationality:	Estonian
E-mail:	siim.kukk@ut.ee

Education

2013–...	University of Tartu, doctoral studies (Chemistry)
2011–2013	University of Tartu, MSc (Chemistry), *cum laude*
2008–2011	University of Tartu, BSc (Chemistry)

Professional employment

2010–…	AS PharmaSynth, Synthetic Chemist, part-time

Scientific publications

Kukk, S.; Stepanov, V.; Järv, J. Thermal Stability of Dopamine Transporters. *J. Membr. Biol.* **2015,** 248, 775–781. https://doi.org/10.1007/s00232-015-9794-9

Kukk, S.; Järv, J. Differentiating between drugs with short and long residence times. *MedChemComm*. **2016**, 7, 1654–1656. https://doi.org/10.1039/C6MD00269B

Kukk, S.; Miidla, P.; Järv, J. Kinetic tools for the identification of ligand – receptor interaction mechanisms. *Proc. Est. Acad. Sci.* **2017**, 66, 202–213. https://doi.org/10.3176/proc.2017.2.08

ELULOOKIRJELDUS

Nimi: Siim Kukk
Sünniaeg: 12.07.1989
Aadress: Keemia instituut, Ravila 14a, 50411, Tartu, Eesti
Kodakondsus: Eesti
E-post: siim.kukk@ut.ee

Haridus

2013–... Tartu Ülikool, doktoriõpe (Keemia)
2011–2013 Tartu Ülikool, MSc (Keemia), *cum laude*
2008–2011 Tartu Ülikool, BSc (Keemia)

Teenistuskäik

2010–… AS PharmaSynth, keemik, osakoormusega

Teaduspublikatsioonid

Kukk, S.; Stepanov, V.; Järv, J. Thermal Stability of Dopamine Transporters. *J. Membr. Biol.* **2015,** 248, 775–781. https://doi.org/10.1007/s00232-015-9794-9

Kukk, S.; Järv, J. Differentiating between drugs with short and long residence times. *MedChemComm*. **2016**, 7, 1654–1656. https://doi.org/10.1039/C6MD00269B

Kukk, S.; Miidla, P.; Järv, J. Kinetic tools for the identification of ligand – receptor interaction mechanisms. *Proc. Est. Acad. Sci.* **2017**, 66, 202–213. https://doi.org/10.3176/proc.2017.2.08

DISSERTATIONES CHIMICAE UNIVERSITATIS TARTUENSIS

1. **Toomas Tamm.** Quantum-chemical simulation of solvent effects. Tartu, 1993, 110 p.
2. **Peeter Burk.** Theoretical study of gas-phase acid-base equilibria. Tartu, 1994, 96 p.
3. **Victor Lobanov.** Quantitative structure-property relationships in large descriptor spaces. Tartu, 1995, 135 p.
4. **Vahur Mäemets.** The ^{17}O and ^{1}H nuclear magnetic resonance study of H_2O in individual solvents and its charged clusters in aqueous solutions of electrolytes. Tartu, 1997, 140 p.
5. **Andrus Metsala.** Microcanonical rate constant in nonequilibrium distribution of vibrational energy and in restricted intramolecular vibrational energy redistribution on the basis of slater's theory of unimolecular reactions. Tartu, 1997, 150 p.
6. **Uko Maran.** Quantum-mechanical study of potential energy surfaces in different environments. Tartu, 1997, 137 p.
7. **Alar Jänes.** Adsorption of organic compounds on antimony, bismuth and cadmium electrodes. Tartu, 1998, 219 p.
8. **Kaido Tammeveski.** Oxygen electroreduction on thin platinum films and the electrochemical detection of superoxide anion. Tartu, 1998, 139 p.
9. **Ivo Leito.** Studies of Brønsted acid-base equilibria in water and non-aqueous media. Tartu, 1998, 101 p.
10. **Jaan Leis.** Conformational dynamics and equilibria in amides. Tartu, 1998, 131 p.
11. **Toonika Rinken.** The modelling of amperometric biosensors based on oxidoreductases. Tartu, 2000, 108 p.
12. **Dmitri Panov.** Partially solvated Grignard reagents. Tartu, 2000, 64 p.
13. **Kaja Orupõld.** Treatment and analysis of phenolic wastewater with microorganisms. Tartu, 2000, 123 p.
14. **Jüri Ivask.** Ion Chromatographic determination of major anions and cations in polar ice core. Tartu, 2000, 85 p.
15. **Lauri Vares.** Stereoselective Synthesis of Tetrahydrofuran and Tetrahydropyran Derivatives by Use of Asymmetric Horner-Wadsworth-Emmons and Ring Closure Reactions. Tartu, 2000, 184 p.
16. **Martin Lepiku.** Kinetic aspects of dopamine D_2 receptor interactions with specific ligands. Tartu, 2000, 81 p.
17. **Katrin Sak.** Some aspects of ligand specificity of P2Y receptors. Tartu, 2000, 106 p.
18. **Vello Pällin.** The role of solvation in the formation of iotsitch complexes. Tartu, 2001, 95 p.
19. **Katrin Kollist.** Interactions between polycyclic aromatic compounds and humic substances. Tartu, 2001, 93 p.

20. **Ivar Koppel.** Quantum chemical study of acidity of strong and superstrong Brønsted acids. Tartu, 2001, 104 p.
21. **Viljar Pihl.** The study of the substituent and solvent effects on the acidity of OH and CH acids. Tartu, 2001, 132 p.
22. **Natalia Palm.** Specification of the minimum, sufficient and significant set of descriptors for general description of solvent effects. Tartu, 2001, 134 p.
23. **Sulev Sild.** QSPR/QSAR approaches for complex molecular systems. Tartu, 2001, 134 p.
24. **Ruslan Petrukhin.** Industrial applications of the quantitative structure-property relationships. Tartu, 2001, 162 p.
25. **Boris V. Rogovoy.** Synthesis of (benzotriazolyl)carboximidamides and their application in relations with *N*- and *S*-nucleophyles. Tartu, 2002, 84 p.
26. **Koit Herodes.** Solvent effects on UV-vis absorption spectra of some solvatochromic substances in binary solvent mixtures: the preferential solvation model. Tartu, 2002, 102 p.
27. **Anti Perkson.** Synthesis and characterisation of nanostructured carbon. Tartu, 2002, 152 p.
28. **Ivari Kaljurand.** Self-consistent acidity scales of neutral and cationic Brønsted acids in acetonitrile and tetrahydrofuran. Tartu, 2003, 108 p.
29. **Karmen Lust.** Adsorption of anions on bismuth single crystal electrodes. Tartu, 2003, 128 p.
30. **Mare Piirsalu.** Substituent, temperature and solvent effects on the alkaline hydrolysis of substituted phenyl and alkyl esters of benzoic acid. Tartu, 2003, 156 p.
31. **Meeri Sassian.** Reactions of partially solvated Grignard reagents. Tartu, 2003, 78 p.
32. **Tarmo Tamm.** Quantum chemical modelling of polypyrrole. Tartu, 2003. 100 p.
33. **Erik Teinemaa.** The environmental fate of the particulate matter and organic pollutants from an oil shale power plant. Tartu, 2003. 102 p.
34. **Jaana Tammiku-Taul.** Quantum chemical study of the properties of Grignard reagents. Tartu, 2003. 120 p.
35. **Andre Lomaka.** Biomedical applications of predictive computational chemistry. Tartu, 2003. 132 p.
36. **Kostyantyn Kirichenko.** Benzotriazole – Mediated Carbon–Carbon Bond Formation. Tartu, 2003. 132 p.
37. **Gunnar Nurk.** Adsorption kinetics of some organic compounds on bismuth single crystal electrodes. Tartu, 2003, 170 p.
38. **Mati Arulepp.** Electrochemical characteristics of porous carbon materials and electrical double layer capacitors. Tartu, 2003, 196 p.
39. **Dan Cornel Fara.** QSPR modeling of complexation and distribution of organic compounds. Tartu, 2004, 126 p.
40. **Riina Mahlapuu.** Signalling of galanin and amyloid precursor protein through adenylate cyclase. Tartu, 2004, 124 p.

41. **Mihkel Kerikmäe.** Some luminescent materials for dosimetric applications and physical research. Tartu, 2004, 143 p.
42. **Jaanus Kruusma.** Determination of some important trace metal ions in human blood. Tartu, 2004, 115 p.
43. **Urmas Johanson.** Investigations of the electrochemical properties of polypyrrole modified electrodes. Tartu, 2004, 91 p.
44. **Kaido Sillar.** Computational study of the acid sites in zeolite ZSM-5. Tartu, 2004, 80 p.
45. **Aldo Oras.** Kinetic aspects of dATPαS interaction with $P2Y_1$ receptor. Tartu, 2004, 75 p.
46. **Erik Mölder.** Measurement of the oxygen mass transfer through the air-water interface. Tartu, 2005, 73 p.
47. **Thomas Thomberg.** The kinetics of electroreduction of peroxodisulfate anion on cadmium (0001) single crystal electrode. Tartu, 2005, 95 p.
48. **Olavi Loog.** Aspects of condensations of carbonyl compounds and their imine analogues. Tartu, 2005, 83 p.
49. **Siim Salmar.** Effect of ultrasound on ester hydrolysis in aqueous ethanol. Tartu, 2006, 73 p.
50. **Ain Uustare.** Modulation of signal transduction of heptahelical receptors by other receptors and G proteins. Tartu, 2006, 121 p.
51. **Sergei Yurchenko.** Determination of some carcinogenic contaminants in food. Tartu, 2006, 143 p.
52. **Kaido Tämm.** QSPR modeling of some properties of organic compounds. Tartu, 2006, 67 p.
53. **Olga Tšubrik.** New methods in the synthesis of multisubstituted hydrazines. Tartu. 2006, 183 p.
54. **Lilli Sooväli.** Spectrophotometric measurements and their uncertainty in chemical analysis and dissociation constant measurements. Tartu, 2006, 125 p.
55. **Eve Koort.** Uncertainty estimation of potentiometrically measured ph and pK_a values. Tartu, 2006, 139 p.
56. **Sergei Kopanchuk.** Regulation of ligand binding to melanocortin receptor subtypes. Tartu, 2006, 119 p.
57. **Silvar Kallip.** Surface structure of some bismuth and antimony single crystal electrodes. Tartu, 2006, 107 p.
58. **Kristjan Saal.** Surface silanization and its application in biomolecule coupling. Tartu, 2006, 77 p.
59. **Tanel Tätte.** High viscosity $Sn(OBu)_4$ oligomeric concentrates and their applications in technology. Tartu, 2006, 91 p.
60. **Dimitar Atanasov Dobchev**. Robust QSAR methods for the prediction of properties from molecular structure. Tartu, 2006, 118 p.
61. **Hannes Hagu**. Impact of ultrasound on hydrophobic interactions in solutions. Tartu, 2007, 81 p.

62. **Rutha Jäger.** Electroreduction of peroxodisulfate anion on bismuth electrodes. Tartu, 2007, 142 p.
63. **Kaido Viht.** Immobilizable bisubstrate-analogue inhibitors of basophilic protein kinases: development and application in biosensors. Tartu, 2007, 88 p.
64. **Eva-Ingrid Rõõm.** Acid-base equilibria in nonpolar media. Tartu, 2007, 156 p.
65. **Sven Tamp.** DFT study of the cesium cation containing complexes relevant to the cesium cation binding by the humic acids. Tartu, 2007, 102 p.
66. **Jaak Nerut.** Electroreduction of hexacyanoferrate(III) anion on Cadmium (0001) single crystal electrode. Tartu, 2007, 180 p.
67. **Lauri Jalukse.** Measurement uncertainty estimation in amperometric dissolved oxygen concentration measurement. Tartu, 2007, 112 p.
68. **Aime Lust.** Charge state of dopants and ordered clusters formation in CaF_2:Mn and CaF_2:Eu luminophors. Tartu, 2007, 100 p.
69. **Iiris Kahn**. Quantitative Structure-Activity Relationships of environmentally relevant properties. Tartu, 2007, 98 p.
70. **Mari Reinik.** Nitrates, nitrites, N-nitrosamines and polycyclic aromatic hydrocarbons in food: analytical methods, occurrence and dietary intake. Tartu, 2007, 172 p.
71. **Heili Kasuk.** Thermodynamic parameters and adsorption kinetics of organic compounds forming the compact adsorption layer at Bi single crystal electrodes. Tartu, 2007, 212 p.
72. **Erki Enkvist.** Synthesis of adenosine-peptide conjugates for biological applications. Tartu, 2007, 114 p.
73. **Svetoslav Hristov Slavov**. Biomedical applications of the QSAR approach. Tartu, 2007, 146 p.
74. **Eneli Härk.** Electroreduction of complex cations on electrochemically polished Bi(*hkl*) single crystal electrodes. Tartu, 2008, 158 p.
75. **Priit Möller.** Electrochemical characteristics of some cathodes for medium temperature solid oxide fuel cells, synthesized by solid state reaction technique. Tartu, 2008, 90 p.
76. **Signe Viggor.** Impact of biochemical parameters of genetically different pseudomonads at the degradation of phenolic compounds. Tartu, 2008, 122 p.
77. **Ave Sarapuu.** Electrochemical reduction of oxygen on quinone-modified carbon electrodes and on thin films of platinum and gold. Tartu, 2008, 134 p.
78. **Agnes Kütt.** Studies of acid-base equilibria in non-aqueous media. Tartu, 2008, 198 p.
79. **Rouvim Kadis.** Evaluation of measurement uncertainty in analytical chemistry: related concepts and some points of misinterpretation. Tartu, 2008, 118 p.
80. **Valter Reedo.** Elaboration of IVB group metal oxide structures and their possible applications. Tartu, 2008, 98 p.

81. **Aleksei Kuznetsov.** Allosteric effects in reactions catalyzed by the cAMP-dependent protein kinase catalytic subunit. Tartu, 2009, 133 p.
82. **Aleksei Bredihhin.** Use of mono- and polyanions in the synthesis of multisubstituted hydrazine derivatives. Tartu, 2009, 105 p.
83. **Anu Ploom.** Quantitative structure-reactivity analysis in organosilicon chemistry. Tartu, 2009, 99 p.
84. **Argo Vonk.** Determination of adenosine A_{2A}- and dopamine D_1 receptor-specific modulation of adenylate cyclase activity in rat striatum. Tartu, 2009, 129 p.
85. **Indrek Kivi.** Synthesis and electrochemical characterization of porous cathode materials for intermediate temperature solid oxide fuel cells. Tartu, 2009, 177 p.
86. **Jaanus Eskusson.** Synthesis and characterisation of diamond-like carbon thin films prepared by pulsed laser deposition method. Tartu, 2009, 117 p.
87. **Marko Lätt.** Carbide derived microporous carbon and electrical double layer capacitors. Tartu, 2009, 107 p.
88. **Vladimir Stepanov.** Slow conformational changes in dopamine transporter interaction with its ligands. Tartu, 2009, 103 p.
89. **Aleksander Trummal.** Computational Study of Structural and Solvent Effects on Acidities of Some Brønsted Acids. Tartu, 2009, 103 p.
90. **Eerold Vellemäe.** Applications of mischmetal in organic synthesis. Tartu, 2009, 93 p.
91. **Sven Parkel.** Ligand binding to 5-HT_{1A} receptors and its regulation by Mg^{2+} and Mn^{2+}. Tartu, 2010, 99 p.
92. **Signe Vahur.** Expanding the possibilities of ATR-FT-IR spectroscopy in determination of inorganic pigments. Tartu, 2010, 184 p.
93. **Tavo Romann**. Preparation and surface modification of bismuth thin film, porous, and microelectrodes. Tartu, 2010, 155 p.
94. **Nadežda Aleksejeva.** Electrocatalytic reduction of oxygen on carbon nanotube-based nanocomposite materials. Tartu, 2010, 147 p.
95. **Marko Kullapere.** Electrochemical properties of glassy carbon, nickel and gold electrodes modified with aryl groups. Tartu, 2010, 233 p.
96. **Liis Siinor.** Adsorption kinetics of ions at Bi single crystal planes from aqueous electrolyte solutions and room-temperature ionic liquids. Tartu, 2010, 101 p.
97. **Angela Vaasa.** Development of fluorescence-based kinetic and binding assays for characterization of protein kinases and their inhibitors. Tartu 2010, 101 p.
98. **Indrek Tulp.** Multivariate analysis of chemical and biological properties. Tartu 2010, 105 p.
99. **Aare Selberg.** Evaluation of environmental quality in Northern Estonia by the analysis of leachate. Tartu 2010, 117 p.
100. **Darja Lavõgina.** Development of protein kinase inhibitors based on adenosine analogue-oligoarginine conjugates. Tartu 2010, 248 p.

101. **Laura Herm.** Biochemistry of dopamine D_2 receptors and its association with motivated behaviour. Tartu 2010, 156 p.
102. **Terje Raudsepp.** Influence of dopant anions on the electrochemical properties of polypyrrole films. Tartu 2010, 112 p.
103. **Margus Marandi.** Electroformation of Polypyrrole Films: *In-situ* AFM and STM Study. Tartu 2011, 116 p.
104. **Kairi Kivirand.** Diamine oxidase-based biosensors: construction and working principles. Tartu, 2011, 140 p.
105. **Anneli Kruve.** Matrix effects in liquid-chromatography electrospray mass-spectrometry. Tartu, 2011, 156 p.
106. **Gary Urb.** Assessment of environmental impact of oil shale fly ash from PF and CFB combustion. Tartu, 2011, 108 p.
107. **Nikita Oskolkov.** A novel strategy for peptide-mediated cellular delivery and induction of endosomal escape. Tartu, 2011, 106 p.
108. **Dana Martin.** The QSPR/QSAR approach for the prediction of properties of fullerene derivatives. Tartu, 2011, 98 p.
109. **Säde Viirlaid.** Novel glutathione analogues and their antioxidant activity. Tartu, 2011, 106 p.
110. **Ülis Sõukand.** Simultaneous adsorption of Cd^{2+}, Ni^{2+}, and Pb^{2+} on peat. Tartu, 2011, 124 p.
111. **Lauri Lipping.** The acidity of strong and superstrong Brønsted acids, an outreach for the "limits of growth": a quantum chemical study. Tartu, 2011, 124 p.
112. **Heisi Kurig.** Electrical double-layer capacitors based on ionic liquids as electrolytes. Tartu, 2011, 146 p.
113. **Marje Kasari.** Bisubstrate luminescent probes, optical sensors and affinity adsorbents for measurement of active protein kinases in biological samples. Tartu, 2012, 126 p.
114. **Kalev Takkis.** Virtual screening of chemical databases for bioactive molecules. Tartu, 2012, 122 p.
115. **Ksenija Kisseljova**. Synthesis of aza-β^3-amino acid containing peptides and kinetic study of their phosphorylation by protein kinase A. Tartu, 2012, 104 p.
116. **Riin Rebane.** Advanced method development strategy for derivatization LC/ESI/MS. Tartu, 2012, 184 p.
117. **Vladislav Ivaništšev.** Double layer structure and adsorption kinetics of ions at metal electrodes in room temperature ionic liquids. Tartu, 2012, 128 p.
118. **Irja Helm.** High accuracy gravimetric Winkler method for determination of dissolved oxygen. Tartu, 2012, 139 p.
119. **Karin Kipper.** Fluoroalcohols as Components of LC-ESI-MS Eluents: Usage and Applications. Tartu, 2012, 164 p.
120. **Arno Ratas.** Energy storage and transfer in dosimetric luminescent materials. Tartu, 2012, 163 p.

121. **Reet Reinart-Okugbeni**. Assay systems for characterisation of subtype-selective binding and functional activity of ligands on dopamine receptors. Tartu, 2012, 159 p.
122. **Lauri Sikk.** Computational study of the Sonogashira cross-coupling reaction. Tartu, 2012, 81 p.
123. **Karita Raudkivi.** Neurochemical studies on inter-individual differences in affect-related behaviour of the laboratory rat. Tartu, 2012, 161 p.
124. **Indrek Saar.** Design of GalR2 subtype specific ligands: their role in depression-like behavior and feeding regulation. Tartu, 2013, 126 p.
125. **Ann Laheäär.** Electrochemical characterization of alkali metal salt based non-aqueous electrolytes for supercapacitors. Tartu, 2013, 127 p.
126. **Kerli Tõnurist.** Influence of electrospun separator materials properties on electrochemical performance of electrical double-layer capacitors. Tartu, 2013, 147 p.
127. **Kaija Põhako-Esko.** Novel organic and inorganic ionogels: preparation and characterization. Tartu, 2013, 124 p.
128. **Ivar Kruusenberg.** Electroreduction of oxygen on carbon nanomaterial-based catalysts. Tartu, 2013, 191 p.
129. **Sander Piiskop.** Kinetic effects of ultrasound in aqueous acetonitrile solutions. Tartu, 2013, 95 p.
130. **Ilona Faustova**. Regulatory role of L-type pyruvate kinase N-terminal domain. Tartu, 2013, 109 p.
131. **Kadi Tamm.** Synthesis and characterization of the micro-mesoporous anode materials and testing of the medium temperature solid oxide fuel cell single cells. Tartu, 2013, 138 p.
132. **Iva Bozhidarova Stoyanova-Slavova.** Validation of QSAR/QSPR for regulatory purposes. Tartu, 2013, 109 p.
133. **Vitali Grozovski**. Adsorption of organic molecules at single crystal electrodes studied by *in situ* STM method. Tartu, 2014, 146 p.
134. **Santa Veikšina**. Development of assay systems for characterisation of ligand binding properties to melanocortin 4 receptors. Tartu, 2014, 151 p.
135. **Jüri Liiv.** PVDF (polyvinylidene difluoride) as material for active element of twisting-ball displays. Tartu, 2014, 111 p.
136. **Kersti Vaarmets.** Electrochemical and physical characterization of pristine and activated molybdenum carbide-derived carbon electrodes for the oxygen electroreduction reaction. Tartu, 2014, 131 p.
137. **Lauri Tõntson**. Regulation of G-protein subtypes by receptors, guanine nucleotides and Mn^{2+}. Tartu, 2014, 105 p.
138. **Aiko Adamson.** Properties of amine-boranes and phosphorus analogues in the gas phase. Tartu, 2014, 78 p.
139. **Elo Kibena**. Electrochemical grafting of glassy carbon, gold, highly oriented pyrolytic graphite and chemical vapour deposition-grown graphene electrodes by diazonium reduction method. Tartu, 2014, 184 p.

140. **Teemu Näykki.** Novel Tools for Water Quality Monitoring – From Field to Laboratory. Tartu, 2014, 202 p.
141. **Karl Kaupmees.** Acidity and basicity in non-aqueous media: importance of solvent properties and purity. Tartu, 2014, 128 p.
142. **Oleg Lebedev**. Hydrazine polyanions: different strategies in the synthesis of heterocycles. Tartu, 2015, 118 p.
143. **Geven Piir.** Environmental risk assessment of chemicals using QSAR methods. Tartu, 2015, 123 p.
144. **Olga Mazina.** Development and application of the biosensor assay for measurements of cyclic adenosine monophosphate in studies of G protein-coupled receptor signalinga. Tartu, 2015, 116 p.
145. **Sandip Ashokrao Kadam.** Anion receptors: synthesis and accurate binding measurements. Tartu, 2015, 116 p.
146. **Indrek Tallo.** Synthesis and characterization of new micro-mesoporous carbide derived carbon materials for high energy and power density electrical double layer capacitors. Tartu, 2015, 148 p.
147. **Heiki Erikson.** Electrochemical reduction of oxygen on nanostructured palladium and gold catalysts. Tartu, 2015, 204 p.
148. **Erik Anderson.** *In situ* Scanning Tunnelling Microscopy studies of the interfacial structure between Bi(111) electrode and a room temperature ionic liquid. Tartu, 2015, 118 p.
149. **Girinath G. Pillai.** Computational Modelling of Diverse Chemical, Bio-chemical and Biomedical Properties. Tartu, 2015, 140 p.
150. **Piret Pikma.** Interfacial structure and adsorption of organic compounds at Cd(0001) and Sb(111) electrodes from ionic liquid and aqueous electrolytes: an *in situ* STM study. Tartu, 2015, 126 p.
151. **Ganesh babu Manoharan.** Combining chemical and genetic approaches for photoluminescence assays of protein kinases. Tartu, 2016, 126 p.
152. **Carolin Siimenson**. Electrochemical characterization of halide ion adsorption from liquid mixtures at Bi(111) and pyrolytic graphite electrode surface. Tartu, 2016, 110 p.
153. **Asko Laaniste.** Comparison and optimisation of novel mass spectrometry ionisation sources. Tartu, 2016, 156 p.
154. **Hanno Evard.** Estimating limit of detection for mass spectrometric analysis methods. Tartu, 2016, 224 p.
155. **Kadri Ligi.** Characterization and application of protein kinase-responsive organic probes with triplet-singlet energy transfer. Tartu, 2016, 122 p.
156. **Margarita Kagan.** Biosensing penicillins' residues in milk flows. Tartu, 2016, 130 p.
157. **Marie Kriisa.** Development of protein kinase-responsive photo-luminescent probes and cellular regulators of protein phosphorylation. Tartu, 2016, 106 p.
158. **Mihkel Vestli.** Ultrasonic spray pyrolysis deposited electrolyte layers for intermediate temperature solid oxide fuel cells. Tartu, 2016, 156 p.

159. **Silver Sepp**. Influence of porosity of the carbide-derived carbon on the properties of the composite electrocatalysts and characteristics of polymer electrolyte fuel cells. Tartu, 2016, 137p.
160. **Kristjan Haav**. Quantitative relative equilibrium constant measurements in supramolecular chemistry. Tartu, 2017, 158 p.
161. **Anu Teearu**. Development of MALDI-FT-ICR-MS methodology for the analysis of resinous materials. Tartu, 2017, 205 p.
162. **Taavi Ivan**. Bifunctional inhibitors and photoluminescent probes for studies on protein complexes. Tartu, 2017, 140 p.
163. **Maarja-Liisa Oldekop**. Characterization of amino acid derivatization reagents for LC-MS analysis. Tartu, 2017, 147 p.
164. **Kristel Jukk**. Electrochemical reduction of oxygen on platinum- and palladium-based nanocatalysts. Tartu, 2017, 250 p.